Stony Brook University

Monomeric Iron and Cobalt Compounds with Cyanide and Isocyanide Ligands

A Thesis Presented

by

Anthony John Pesiri

to

The Graduate School

in Partial Fulfillment of the

Requirements

for the Degree of

Master of Science

in

Chemistry

Stony Brook University

August 2009

Stony Brook University

The Graduate School

Anthony John Pesiri

We, the thesis committee for the above candidate for the

Master of Science degree, hereby recommend

acceptance of this thesis.

Dr. Stephen Koch - Thesis Advisor
Professor of Chemistry

Dr. Joseph Lauher - Chairperson of Defense
Professor of Chemistry

Dr. David Hanson – Third Member
Professor of Chemistry

This thesis is accepted by the Graduate School

Lawrence Martin
Dean of the Graduate School

Abstract of the Thesis

Monomeric Iron and Cobalt Compounds with Cyanide and Isocyanide Ligands

by

Anthony John Pesiri

Master of Science

in

Chemistry

Stony Brook University

2009

Hydrogen power is a tremendous area of research today as there are almost endless amounts of possible applications to this type of clean alternative to almost every other type of power. The seemingly simple act of reducing protons to Hydrogen gas cleanly, efficiently and in significant quantities has proven difficult. However, there is a known class of proteins that are able to do this very well: Hydrogenases.

The goal of this research is to investigate and synthesize different types of molecules that essentially mimic the protein backbone and metal centers of Hydrogenase by utilizing the bulky chelating ligand known as *tris*(2-thiophenyl)phosphine, or more simply as H_3PS3 as the backbone. The metal center is mimicked by attaching this ligand to a different metal centers to create monomers or dimers. While dimeric compounds have been synthesized, the focus of this research is on various monomeric iron and cobalt compounds complexed with the H_3PS3 ligand along with differing types of cyanide and isocyanide ligands. These monomeric molecules show promise in one day being able to reduce protons to Hydrogen gas, due to the fact that the iron especially the cobalt compounds are easily oxidized. That important property is why these molecules show great promise in utilizing them in order to reduce protons to Hydrogen gas.

Table of Contents

List of Figures

List of Tables

List of Abbreviations

Bz	Benzyl
CV	Cyclic Voltammogram
DMSO	Dimethyl Sulfoxide
Equiv	Equivalents
IR	Infrared
Me	Methyl
MeOH	Methanol
NMR	Nuclear Magnetic Resonance
Ph	Phenyl
ppm	Parts Per Million
H_3(PS3)	Tris(2-thiophenyl)phosphine

Introduction

Hydrogenases are extremely important in reactions involving hydrogen production and consumption. They catalyze the reversible reaction of interconverting hydrogen to protons and electrons as shown:

$$H_2 \rightleftharpoons 2H^+ + 2e^-$$

Hydrogenases allow this reaction to occur at a measurable rate and it is essential to the healthy function of all living organisms. In the field of chemistry, hydrogenase is valuable because of its ability to catalyze this extremely important reaction that is being utilized in many types of biochemical fuel cells, such as solar cells. It is also highly sought after by inorganic chemists to synthesize molecules that can mimic the active sites in order to understand how the enzyme works and to tailor it to specific conditions and functions.

There are a few types of hydrogenases: a Ni-Fe, a mono Fe, and an Fe-Fe center.

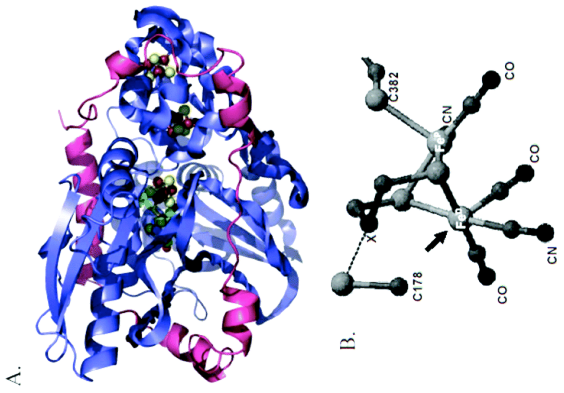

Fig 1. A. Fe-Fe Hydrogenase B. Fe-Fe core and active site

The classes of hydrogenases have differing effects as to which direction this reaction is favored. While the main types of hydrogenases are listed here, there are many variations of these major types that are specific to the many organisms where these classes of enzymes are present.

A major problem with hydrogenases is inhibition at the active site. O_2 or CO, especially, can irreversibly bind and "overcoming inhibition or permanent damage is a challenge for microbes, as well as for future technologies aiming to exploit or mimic these catalysts for electrochemical hydrogen cycling or improve them for biological H_2 production."[1] This is an important factor and must be taken into account when designing a mechanism or a molecule to either mimic the active site of a specific type of hydrogenase or making a biological fuel cell.

Michael Hambourger *et. al.* created a biochemical fuel cell utilizing Fe-Fe hydrogenase, which was "adsorbed to pyrolytic graphite edge and carbon felt electrodes. Cyclic voltammograms of the immobilized hydrogenase films reveal cathodic proton reduction and anodic hydrogen oxidation, with a catalytic bias toward hydrogen evolution."[2]

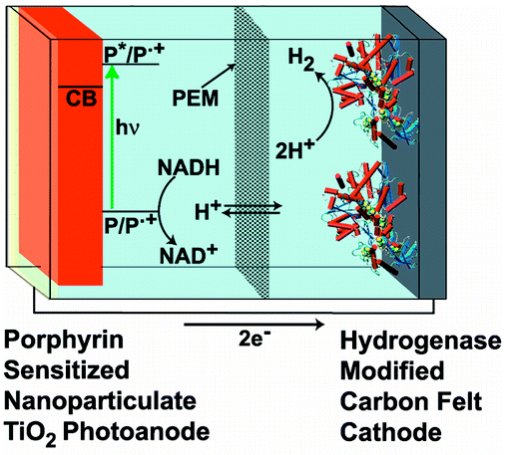

Fig 2. The mechanism and medium of a fuel cell.

These fuel cells are used to harness solar power by coupling photochemistry with hydrogenase to catalyze the reaction.

Researchers are attempting not only to understand how and why the enzyme catalyzes this very important reaction, but are also now trying to mimic the active site of Fe-Fe hydrogenase in many ways. Synthetic chemists are utilizing different metals to achieve the same results as the natural enzyme. The benefits of this are great in terms of advancing hydrogen power to create next generation fuel cells. Liu and Darensbourg of Texas A&M University produced a mixed valence Fe(I)Fe(II) compound that effectively mimics the active site's unique rotated state.

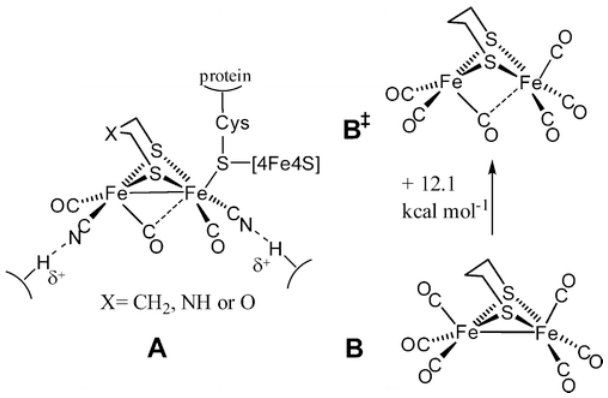

Fig 3. Fe-Fe Hydrogenase and an analog

A. Fe-Fe hydrogenase B. The synthesized analog.

The authors stated that their analog's active site is "readily activated by redox changes to perform both hydrogenase functions, H^+ reduction, and H_2 binding and oxidation."[3] Here is an example of a working analog that can perform functions similar to that of Fe-Fe hydrogenase. In fact, the Fe-Fe hydrogenase is more easily able to be mimicked than the other types. The reason behind this is because the Fe-Fe active site "has proven more amenable to synthetic model studies due to its resemblance to the well-known organometallic complex (μ-pdt)$[Fe(CO)_3]_2$ (pdt = propanedithiolate)."[4] While hydrogenase itself has been adapted into fuel cells as was seen before, the ability to adapt a synthetic molecule that can be cheaper to produce as well as easier to incorporate into a system such as this due to the absence of a large protein structure.

Other studies of hydrogenase active site function also show some interesting results when substituting hydrides in certain places on the Fe-Fe center. "The protonation at a single Fe center conforms to a mechanism whereby proton reduction, hydrogen oxidation, and CO inhibition all occur via substrate binding at a single site on the distal Fe."[5] Also, the charge on Fe-Fe center plays a big role in whether or not H_2 can be

produced. The following diagram shows that a positively charged Fe-Fe center will not afford hydrogen production, but if the overall molecule is neutral hydrogen will be produced.[5]

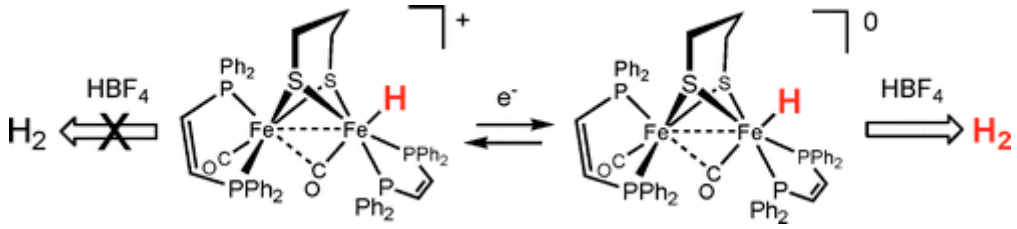

Fig 4. Activity of Synthetic Analog of Fe-Fe Hydrogenase in H_2 Production.

It is important to note that the "protonation of diiron dithiolato complexes can occur at a single Fe site, even for symmetrical $(Fe^{I})_2$ compounds" because the enzyme will only work in a certain way, and this finding helps us to understand hydrogenase function. This is because it gives a clue to how hydrogen would bind to the actual enzyme. The study of how hydrogen binds also showed that "isomerization of the terminal hydride is inhibited both by the basicity of the Fe_2 complex as well as by the steric size of the dithiolate in the models."[5] Since the analog is similar to that of the enzyme, it can be assumed that the reason for the inability of isomerization of the hydride in the enzyme also has to do with steric factors along with others. In the enzyme, "terminal-bridge isomerization may also be inhibited by hydrogen bonding between CN_{distal} and a ϵ-ammonium center of a nearby, highly conserved lysine residue."[5] Due to both the sterics as well as the chemical properties of the amino acid residues, the terminal hydride cannot isomerize in the actual enzyme for more reasons than in the analog. In the analogs, the bulky thiolate groups compensate for the sterics, but not for the chemical factors.

Research into hydrogenase has come a long way and the enzyme is still yet to be completely understood. The active site of Fe-Fe hydrogenase has been successfully mimicked in more than one case and many different types of analogs have been produced. The amount of possible applications for hydrogenase and its many synthetic analogs are quite vast, and are likely to play a tremendous role in the hydrogen powered fuel cells of the future.

Previous Work with the PS3 Ligand

The Millar group has extensively investigated nickel complexes with the tetradentate ligand, H_3(PS3).

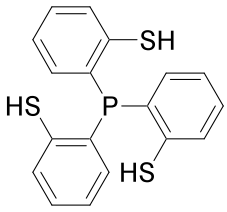

Fig 5. H_3(PS3) ligand

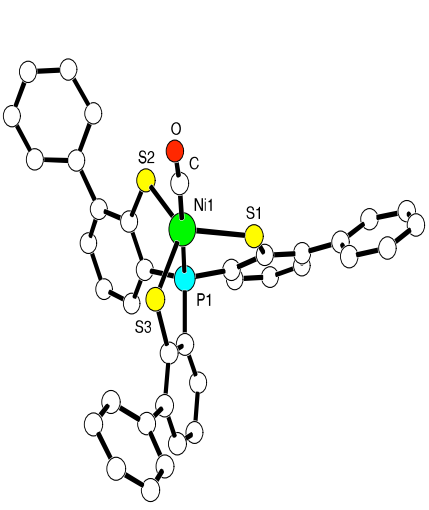

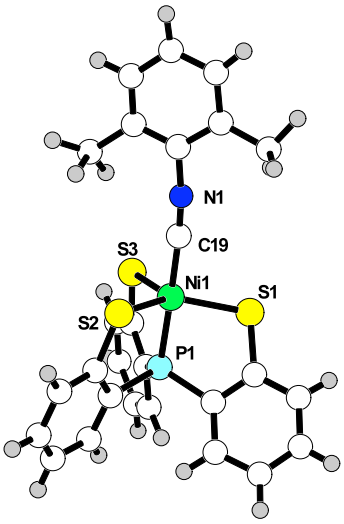

Fig. 6 and 7. [(PS3)Ni^{II,III}(CO)]$^{n-}$ and [(PS3)Ni^{II,III}(2,6-dimethylphenylisocyanide)]$^{n-}$

Monomeric complexes included $[(PS3)Ni^{II,III}(L)]^{n-}$ complexes where L is CO, pyridine, 1-methylimidazole and 2,6-dimethylphenylisocyanide. All the monomeric complexes were five coordinate trigonal bipyramidal with the L ligands trans to P (**Figures 6 and 7).**

The Koch group has extensively studied iron complexes with the PS3 ligand. In addition to trigonal bipyramidal structures such as $[(PS3)Fe^{II}(CO)]^{1-}$, $[(PS3)Fe^{II,III}(CN)]^{2-,1-}$ and [(PS3)Fe(NO)], octahedral complexes have been structurally characterized: $[(PS3)Fe^{II}(CO)_2]^{1-}$. $[(PS3)Fe^{II,III}(CN)(CO)]^{2-,1-}$ and $[(PS3)Fe^{III}(CN)_2]^{2-}$.

The aim of this thesis was to begin to explore the related chemistry of cobalt with this

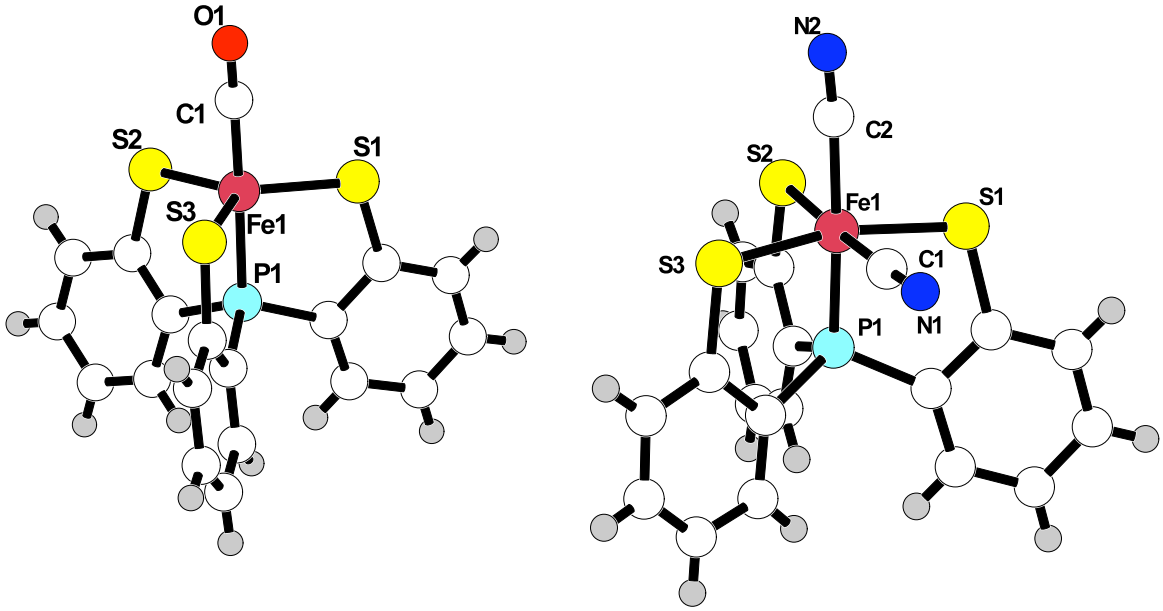

Fig 8 and 9. $[(PS3)Fe^{II}(CO)]^{1-}$ and $[(PS3)Fe^{III}(CN)_2]^{2-}$.

PS3 ligand. Previous to this work, there were no examples of related cobalt compounds. We are interested in exploring the difference in the structural, spectroscopic and reactivity properties of complexes of Fe, Co and Ni with similar or identical ligand sets.

Experimental Techniques

Synthetic Techniques

All reactions were performed under standard Schlenk conditions under a nitrogen atmosphere. All air-sensitive solids were transferred to other medium via a glove box, also under a nitrogen atmosphere.

Instrumentation

Infrared Spectroscopy

All infrared spectra were recorded on a Thermo Scientific nicolet iS10 FTIR spectrometer. All reported spectra were taken using samples in the solid state as KBR pellets.

NMR Spectroscopy

All ^{1}H NMR and ^{31}P NMR spectroscopy were recorded on a Varian Gemini 2300 spectrometer at 300 MHz. All spectra were taken in deuterated solvent and reported in units of parts per million (ppm). All ^{13}C NMR spectra were taken on a Varian Gemini 2300 spectrometer at 400MHz. All spectra were taken in deuterated solvent and reported in units of parts per million (ppm).

Electrochemistry

Electrochemical studies were performed under a nitrogen atmosphere, except where noted, and were carried out on a BAS 100B electrochemical analyzer. All experimental concentrations of were 5mM, with a 10mM concentration of the supporting

electrolyte $[Bu_4N][BF_4]$. Both a platinum and a glassy carbon electrode were utilized as the working electrode in these studies to see which gave a better spectrum. The reference electrode was composed of Ag/AgCl, with the auxiliary electrode being composed of platinum.

Electronic Spectroscopy (UV-VIS)

For UV-VIS studies, an HP 8453 UV-Visible Spectrophotometer was utilized. A tungsten lamp was used for the visible region and a deuterium lamp for the ultraviolet region. All samples were prepared at a 5mM concentration in quartz UV-VIS cells. Each experiment was comprised of two solutions, with pathlengths of 0.1mm and 1.0mm.

X-ray Crystallography

All reported X-ray crystallography studies were performed with an Oxford Diffraction Gemini Diffractometer, utilizing Molybdenum radiation. Some structures were done at low temperature and is indicated in the individual compound data located in the appendix. Data reduction was performed with CrysalisPro software, and the structures were solved using Wingx, Shelx and SIR2004.

Experimental

*All experiments and steps were performed under a nitrogen atmosphere unless otherwise noted.

$[Me_3NBz]_2[Co^{III}(PS3)(CN)_2]$ (1)

H_3PS3 (0.2g, 0.55mmol), Li wire (0.014, 0.165mmol), $CoCl_2 \bullet 6H_2O$ (0.13g, 0.55mmol), and NaCN (0.550.11g, mmol) were added to an RBF and 30 mL of methanol was transferred in via cannula. All of the reagents were stirred until dissolved over a period of an hour and a half to yield a red solution. The mixture was then filtered slowly through celite into another RBF containing the cation $[Me_3NBz]Br$, which was dissolved in a minimum amount of methanol. This new solution quickly formed a red microcrystalline precipitate to give 0.11g at 26% yield.

IR (KBr): $\nu_{CN} = 2089cm^{-1}, 2112cm^{-1}$

^{1}H NMR (DMSO-d_6): δ (ppm) 3.57 (s, 18H), 4.90 (s, 4H)

^{31}P NMR (DMSO-d_6): δ (ppm) 131

^{13}C NMR (DMSO-d_6): δ (ppm) 52, 68, 163.81 ($^2J_{P-C}$ 33.0Hz), 164.71 ($^2J_{P-C}$ 31.7Hz)

UV-VIS (CH_2Cl_2): λ_{max} (ε_m) = 493 (986), 575 (1150), 399 (7980)

X-ray crystal Structure: Single crystals of X-ray quality were grown via a vapor diffusion of acetonitrile/toluene. The crystals were red in color. See Appendix for detailed crystal data.

Co^{III}(PS3)(CN-Me_2Ph)$_2$ (2)

H_3PS3 (0.2g, 0.55mmol), Li wire (0.014g 0.165mmol), $CoCl_2$•$6H_2O$ (0.13g 0.55mmol), and 5 equiv of 2,6-dimethylphenyl isocyanide (Me_2PhNC) (0.363g 0.55mmol), were added to an RBF. 30 mL of methanol was then transferred in via cannula. All the reagents were stirred and dissolved to form a dark purple mixture over a period of an hour a powdery, precipitate formed. This was then filtered to yield a bluish-purple powder to give 0.18g at 49% yield.

*This synthesis can also be completed utilizing a stepwise procedure, as shown below. The following three syntheses can also be performed under similar stepwise manners:

$CoCl_2$ (0.13g, 0.55mmol) was added dropwise to 3 equiv of Li wire (0.014g, 0.165mmol), pre-dissolved in methanol with H_2PS3 (0.2g, 0.55mmol) under nitrogen and allowed to stir for 15 minutes. 5 equiv of 2,6-dimethylphenyl isocyanide (Me_2PhNC) (0.363g, 0.275mmol) dissolved in degassed methanol was added dropwise to the reaction mixture. A large amount of bluish-purple microcrystalline and powdery precipitate was formed.

IR (KBr): ν_{CN} = 2162cm^{-1}, 2175cm^{-1}

^{1}H NMR (DMSO-d_6): δ (ppm) 1.88 (s, 9H), 2.55 (s, 9H)

^{31}P NMR (DMSO-d_6): δ (ppm) 131

^{13}C NMR ($CDCl_3$): δ (ppm) 18, 19.5, 157.06 ($^2J_{P\text{-}C}$ 27.9Hz), 159.65 ($^2J_{P\text{-}C}$ 26.2Hz)

UV-VIS (CH_2Cl_2): λ_{max} (ε_m) = 519 (1038), 279 (5580), 325 (6500)

X-ray crystal Structure: Single crystals of X-ray quality were grown via a vapor diffusion of methylene chloride/pentane. The crystals were green in color. See Appendix for detailed crystal data.

$Co^{III}(PS3)(CNC(CH_3)_3)_2$ (3)

H_3PS3 (0.2g, 0.55mmol), Li wire (0.014g, 0.165mmol), $CoCl_2 \bullet 6H_2O$ (0.13g, 0.55mmol), and 4 equiv of *t*-butyl isocyanide ($(CH_3)_3CNC$) (0.25 mL, 0.55mmol), were added to an RBF. 30 mL of methanol was then transferred in via cannula. All the reagents were stirred and dissolved to form a dark purple solution. Over the period of an hour, a powdery precipitate formed. This was then filtered to yield a dark purple powder to give 0.12g at 41% yield.

IR (KBr): $\nu_{CN} = 2166cm^{-1}, 2184cm^{-1}$

^{1}H NMR (DMSO-d_6): δ (ppm) 0.80 (s, 9H), 1.65 (s, 9H)

^{31}P NMR (DMSO-d_6): δ (ppm) 131

^{13}C NMR (DMSO-d_6): δ (ppm) 28.5, 30, 56, 59, 158.58ppm ($^{2}J_{P\text{-}C}$ 29.0Hz), 159.17ppm ($^{2}J_{P\text{-}C}$ 26.3Hz)

UV-VIS (CH_2Cl_2): λ_{max} (ε_m) = 285 (5700), 314 (6280), 391 (7820), 485 (782), 568 (1136)

X-ray Crystal Structure: Single crystals of X-ray quality were grown via a vapor diffusion of acetonitrile/ether. The crystals were dark purple in color. See Appendix for detailed crystal data.

Fe^{III}(PS3)(CN-Me_2Ph)$_2$ (4)

H_3PS3 (0.2g, 0.55mmol), Li wire (0.014g 0.165mmol), $FeCl_2$•$2H_2O$ (0.11g 0.55mmol), and 5 equiv of 2,6-dimethylphenyl isocyanide (Me_2PhNC) (0.363g 0.55mmol), were added to an RBF. 30 mL of methanol was then transferred in via cannula. All the reagents were stirred and dissolved to form a red solution. Over the period of an hour a powdery precipitate formed. This was then filtered and dried open to air, to yield a bright red-brown powder to give 0.05g at 13% yield.

IR (KBr): ν_{CN} = 2130cm^{-1}, 2154cm^{-1}

CV (5mM in Methylene chloride with 0.10M [Bu_4N][BF_4], Pt electrode, vs. SCE):

$E_{1/2}$ (ΔEp) = -0.135V (60mV) vs. Ag/AgCl

UV-VIS (CH_2Cl_2): λ_{max} (ε_m) = 281 (5620), 550 (1100)

X-ray Crystal Structure: Single crystals of X-ray quality were grown via a vapor diffusion of methylene chloride/pentane. The crystals were dark purple in color. See Appendix for detailed crystal data.

Fe^{III}(PS3)(CNC(CH_3)$_3$)$_2$ (5)

H_3PS3 (0.2g, 0.55mmol), Li wire (0.014g 0.165mmol), $FeCl_2$•$2H_2O$ (0.11g 0.55mmol), and 5 equiv of tert-butyl isocyanide ((CH_3)$_3$CNC) (0.25 ml 0.18g 0.55mmol), were added to an RBF. 30 mL of methanol was then transferred in via cannula. All the reagents were stirred and dissolved to form an olive-green solution. This was allowed to stir for a half hour then exposed to air five times, and stirred open to air for another hour.

Over this period a precipitate formed, which was also filtered open to air and dried and stored under air, giving a red-brown powder to give 0.06g at 19% yield.

IR (KBr): ν_{CN} = 2142cm^{-1}, 2158cm^{-1}

CV (5mM in methylene chloride with 0.10M [Bu_4N][BF_4], Pt electrode, vs. SCE):

$E_{1/2}$ (ΔEp) = -0.260V (60mV) vs. Ag/AgCl

UV-VIS (CH_2Cl_2): λ_{max} (ε_m) = 272 (5440), 540 (1080)

X-ray Crystal Structure: Single crystals of X-ray quality were grown via a vapor diffusion of methylene chloride/ether. The crystals were dark purple in color. See Appendix for detailed crystal data.

Results and Discussion

Chemistry of $[Me_3NBz]_2[Co^{III}(PS3)(CN)_2]$ (1)

[$Co^{III}(PS3)(CN)_2]^{2-}$ was synthesized by lithiating the H_3PS3 ligand in methanol, which would then react with $CoCl_2$ and NaCN to form **1**. All reagents can be added and stirred together from the beginning of the reaction, as performing the reaction in this fashion or in a stepwise manner will produce the same results. This compound is similar to **[**$Fe^{III}(PS3)(CN)_2]^{2-}$compound which was prepared and characterized by Acunzo and Jiang. the difference being that cobalt is the metal center utilized instead of iron. The crystal structure reveals that this compound has an octahedral cobalt center, with three thiolate sulfurs occupying the equatorial positions of the molecule, the phosphorous in an axial position, and the cyanides occupying both an axial and equatorial position.

Table 1. Bond distances and Bond Angles for $[Me_3NBz]_2[Co^{III}(PS3)(CN)_2]$ (1)

Bond Distances (Å)		**Bond Angles** (Deg)	
Co(1)-C(2)	1.8769(17)	P(1)-Co(1)-S(1)	87.78(2)
Co(1)-C(1)	1.9302(18)	C(2)-Co(1)-C(1)	90.19(7)
Co(1)-P(1)	2.1167(8)	C(2)-Co(1)-P(1)	95.42(5)
Co(1)-S(1)	2.2652(8)	C(1)-Co(1)-P(1)	173.31(5)
Co(1)-S(2)	2.2776(10)	C(2)-Co(1)-S(1)	86.16(6)
Co(1)-S(3)	2.3241(8)	C(1)-Co(1)-S(1)	88.96(5)

P(1)-C(4)	1.8007(16)	P(1)-Co(1)-S(1)	87.78(2)
P(1)-C(16)	1.8045(17)	C(2)-Co(1)-S(2)	175.35(5)
P(1)-C(10)	1.8113(16)	C(1)-Co(1)-S(2)	86.03(5)
S(1)-C(3)	1.7513(18)	P(1)-Co(1)-S(2)	88.54(2)
S(2)-C(9)	1.7472(18)	S(1)-Co(1)-S(2)	96.45(3)
S(3)-C(15)	1.7616(18)	C(2)-Co(1)-S(3)	86.58(5)
C(1)-N(1)	1.157(2)	C(1)-Co(1)-S(3)	102.72(5)
C(2)-N(2)	1.1595(19)	P(1)-Co(1)-S(3)	81.31(2)

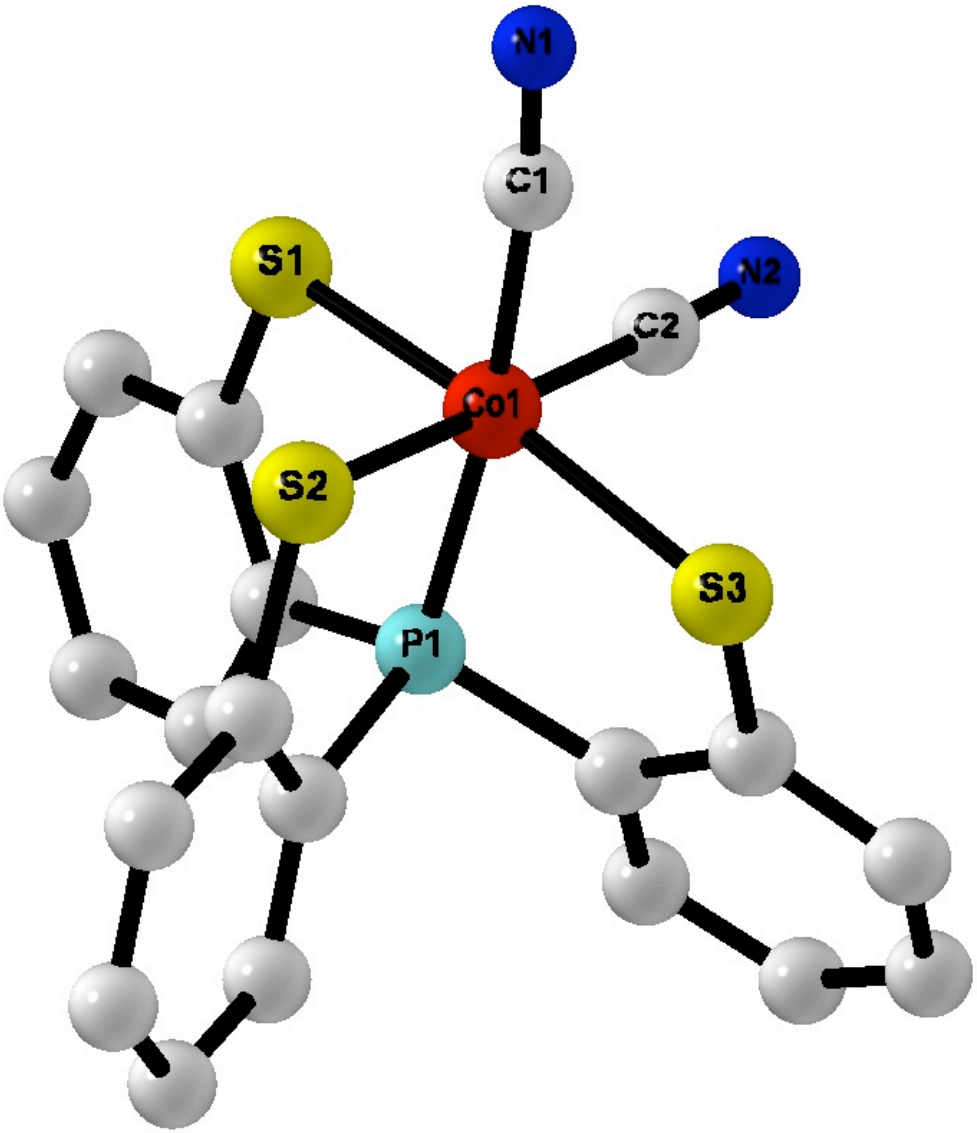

Fig 10. CHARON diagram of $[Me_3NBz]_2[Co^{III}(PS3)(CN)_2]$ (1)

The IR stretching frequencies for compound **1** in the solid state are 2089cm^{-1} and 2112cm^{-1} were higher in energy than its iron analog, $[PPh_4]_2[Fe^{III}(PS3)(CN)_2]$ synthesized by Acunzo[6], which were located at 2076cm^{-1} and 2084cm^{-1}. This agrees with the trend that will be seen multiple times, showing that cobalt analogs of these compounds compared to their iron versions tend to exhibit IR spectra that where the two ligand peaks

appear at higher wavenumbers. The IR shows two peaks of nearly equal intensity, indicating two cyanide ligands are attached to the cobalt, which was proven with the compound's crystal structure.

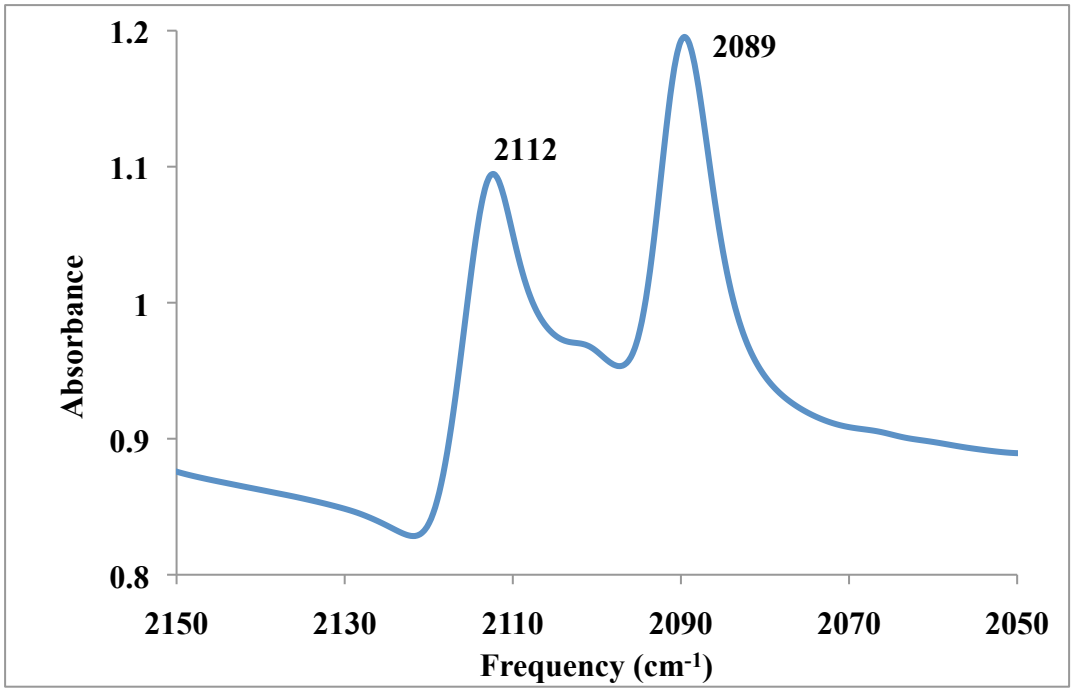

Fig 11. IR spectrum (KBr) of $[Me_3NBz]_2[Co^{III}(PS3)(CN)_2]$ (1)

The ^{1}H NMR spectrum of **1** indicates it is a diamagnetic structure: The integration for the protons in the aromatic region comes out to 12, which is expected for this structure and ^{31}P NMR spectroscopy also gave a single resonance. The compound's ^{13}C NMR with assignments to some peaks is shown in figure 13. The two doublets at 164.71PPM ($^{2}J_{P\text{-}C}$ 31.7Hz) and 163.81PPM ($^{2}J_{P\text{-}C}$ 33.0Hz) are assigned to the cyanide carbons.

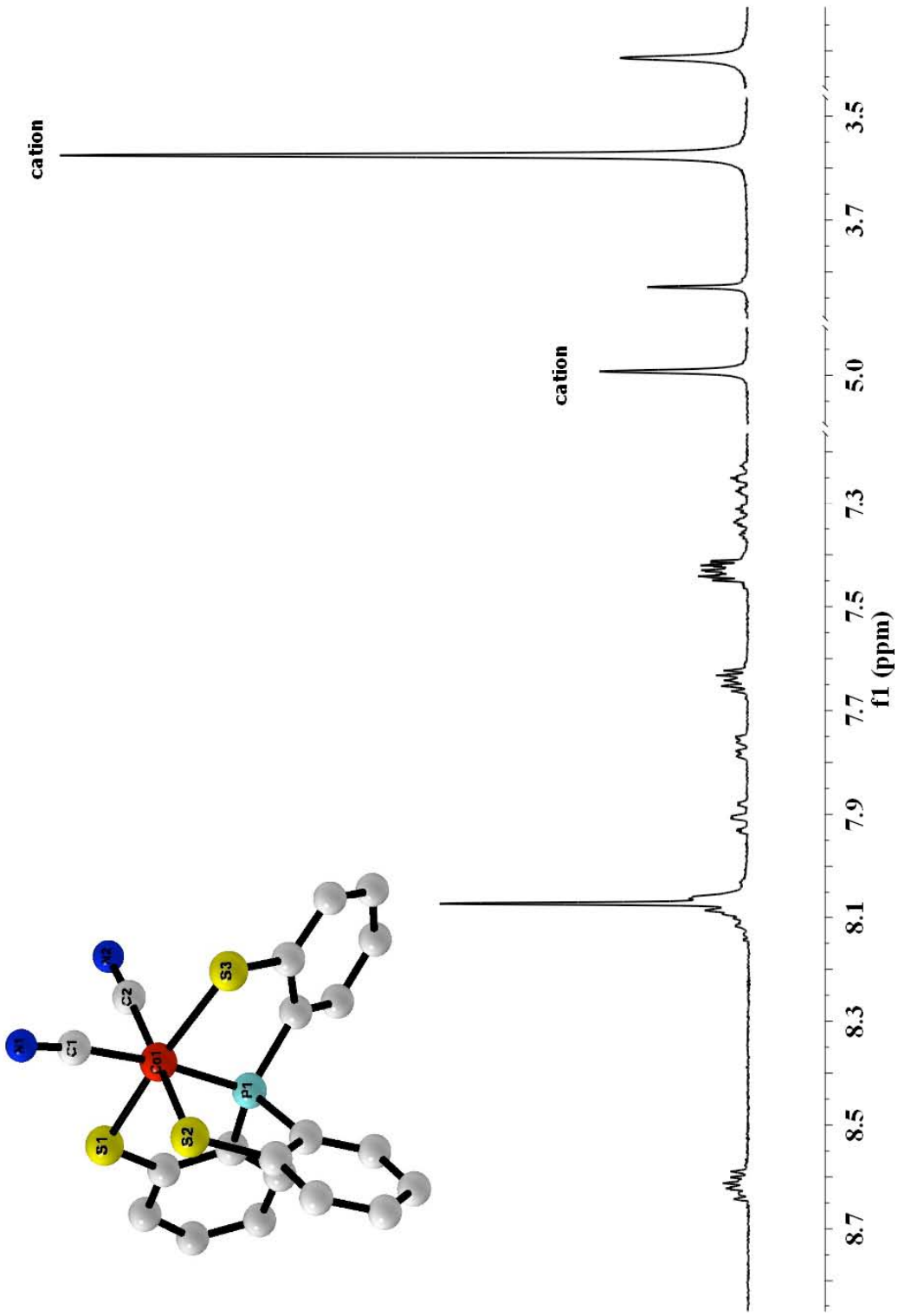

Fig 12. ^{1}H NMR spectrum of $[Me_3NBz]_2[Co^{III}(PS3)(CN)_2]$ (1)

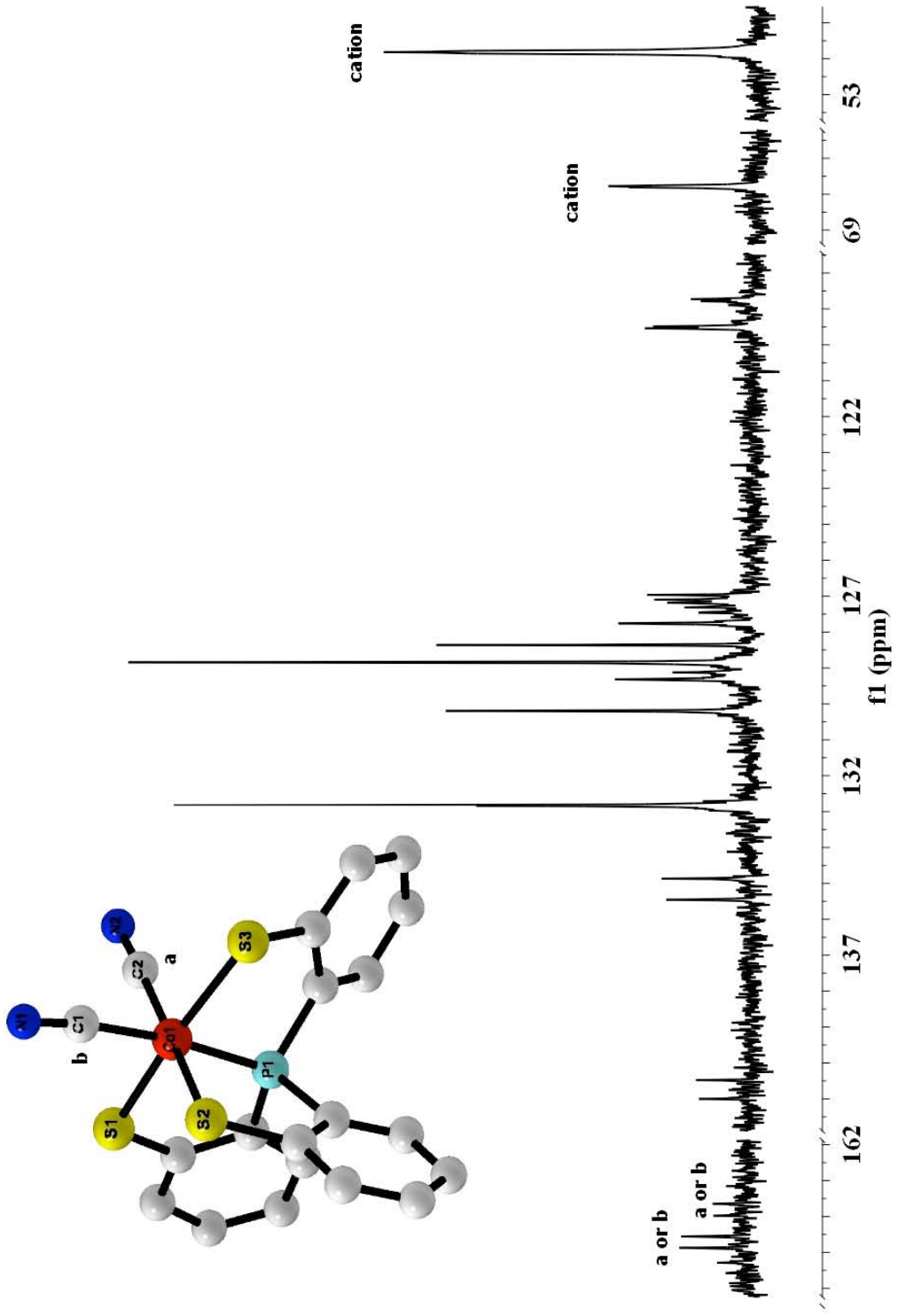

Fig 13. ^{13}C NMR spectrum of $[Me_3NBz]_2[Co^{III}(PS3)(CN)_2]$ (1)

Electrochemical studies of **1** showed no reversible or irreversible peaks, thus were inconclusive and are not shown.

The UV VIS spectrum for this compound is shown below:

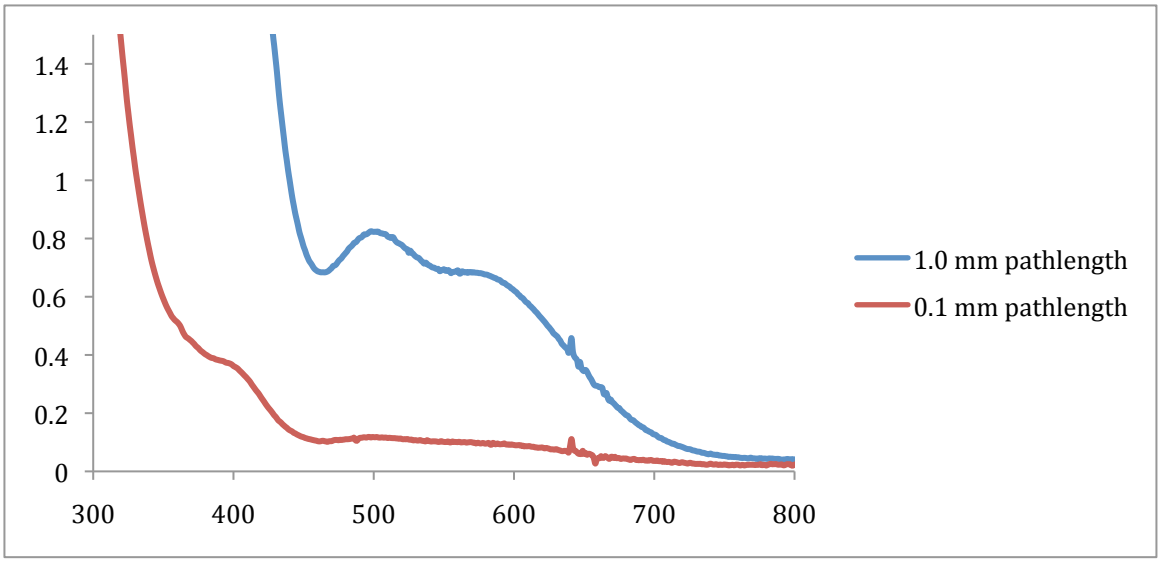

Fig 14. UV-VIS spectrum of $[Me_3NBz]_2[Co^{III}(PS3)(CN)_2]$ (1)

Chemistry of $Co^{III}(PS3)(CN\text{-}Me_2Ph)_2$ (2)

$Co^{III}(PS3)(CN\text{-}Me_2Ph)_2$ was synthesized by lithiating the H_3PS3 ligand in methanol, which would then react with $CoCl_2$ and 2,6-dimethylphenyl isocyanide to form **2**. All reagents can be added and stirred together from the beginning of the reaction, as performing the reaction in this fashion or in a stepwise manner will produce the same results. This compound is very similar to that of its iron counterpart, $Fe^{III}(PS3)(CN\text{-}Me_2Ph)_2$, of which their similarities will be discussed later. The crystal structure of **2** revealed that it had an octahedral cobalt center, with three thiolate sulfurs occupying the equatorial positions of the molecule, the phosphorous in an axial position, and the dimethylphenyl isocyanide ligands occupying both an axial and equatorial position. The crystal structure's bond distances, bond angles, and picture are shown below.

Table 2. Bond distances and Bond Angles for $Co^{III}(PS3)(CN\text{-}Me_2Ph)_2$ (2)

Bond Distances (Å)		**Bond Angles (Deg)**	
Co(1)-C(2)	1.838(2)	C(2)-Co(1)-C(1)	86.66(8)
Co(1)-C(1)	1.891(2)	C(2)-Co(1)-P(1)	95.31(6)
Co(1)-P(1)	2.1402(5)	C(1)-Co(1)-P(1)	176.49(6)
Co(1)-S(2)	2.2708(6)	C(2)-Co(1)-S(2)	174.81(6)
Co(1)-S(3)	2.2835(6)	C(1)-Co(1)-S(2)	88.65(6)
Co(1)-S(1)	2.2901(6)	P(1)-Co(1)-S(2)	89.49(2)
S(1)-C(3)	1.753(2)	C(2)-Co(1)-S(3)	88.29(6)

S(2)-C(9)	1.747(2)	C(1)-Co(1)-S(3)	92.81(6)
S(3)-C(15)	1.752(2)	P(1)-Co(1)-S(3)	84.356(19)
P(1)-C(10)	1.8001(19)	S(2)-Co(1)-S(3)	94.16(3)
P(1)-C(16)	1.805(2)	C(2)-Co(1)-S(1)	85.21(6)
P(1)-C(4)	1.8089(16)	C(1)-Co(1)-S(1)	96.90(6)
C(1)-N(1)	1.145(2)	P(1)-Co(1)-S(1)	86.18(2)
C(2)-N(2)	1.147(2)	S(2)-Co(1)-S(1)	93.16(3)
		S(3)-Co(1)-S(1)	167.97(2)

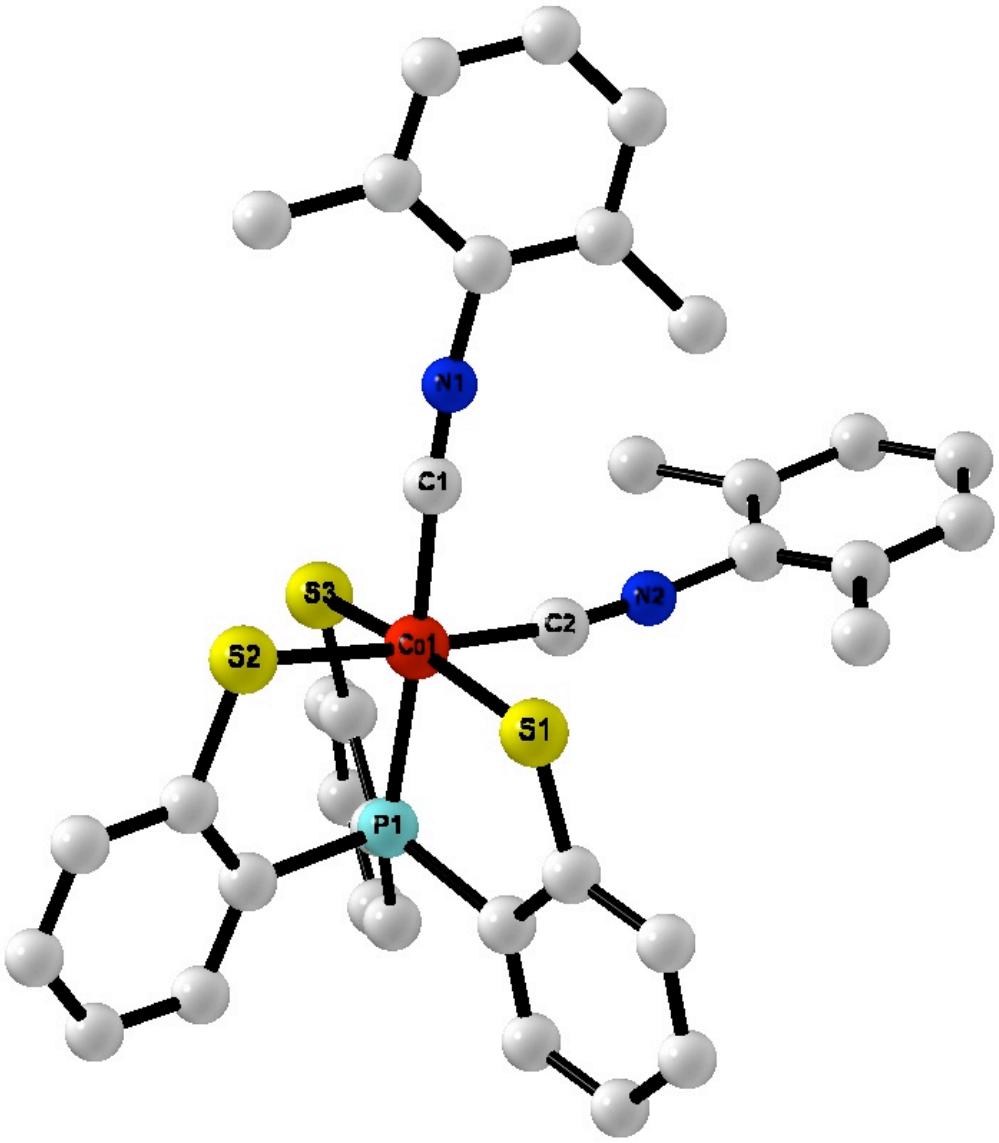

Fig 15. CHARON diagram of $Co^{III}(PS3)(CN\text{-}Me_2Ph)_2$ (2)

The IR stretching frequencies for **2** in the solid state are 2162cm^{-1} and 2175cm^{-1}. The IR shows two peaks of nearly equal intensity, indicating two dimethylphenyl isocyanide ligands are attached to the cobalt, which was proven with the compound's crystal structure.

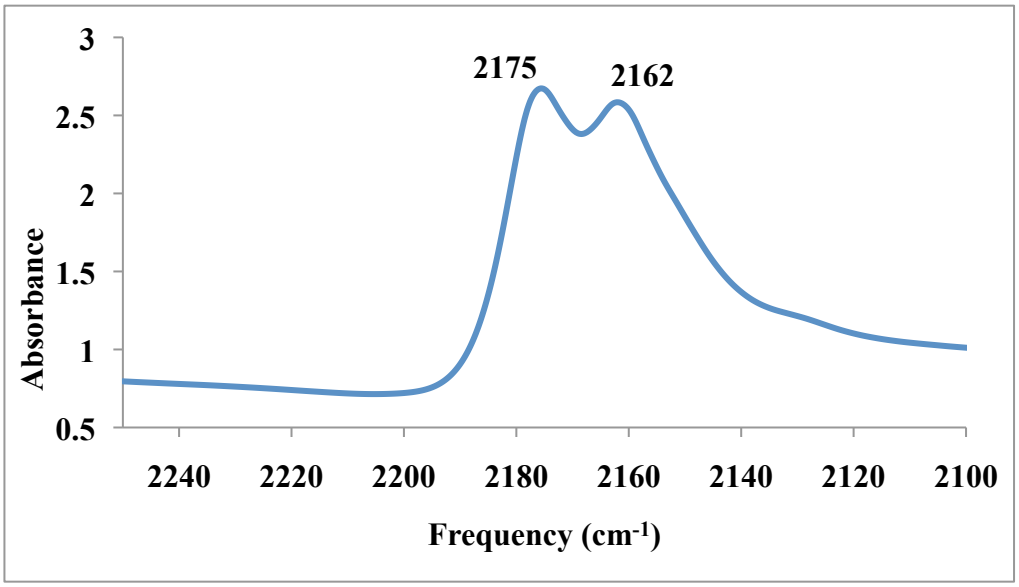

Fig 16. IR spectrum (KBr) of $Co^{III}(PS3)(CN\text{-}Me_2Ph)_2$ (2)

The ^{1}H NMR spectrum of **2** indicates it is a diamagnetic structure. ^{31}P NMR spectroscopy gave a clean spectrum with only one peak appearing at 131ppm. The ^{13}C NMR spectrum with assignments to some peaks is shown in figure 18. The two doublets at 159.65PPM ($^{2}J_{P\text{-}C}$ 26.2Hz) and 157.06PPM ($^{2}J_{P\text{-}C}$ 27.9Hz) are assigned to the isocyanide carbons.

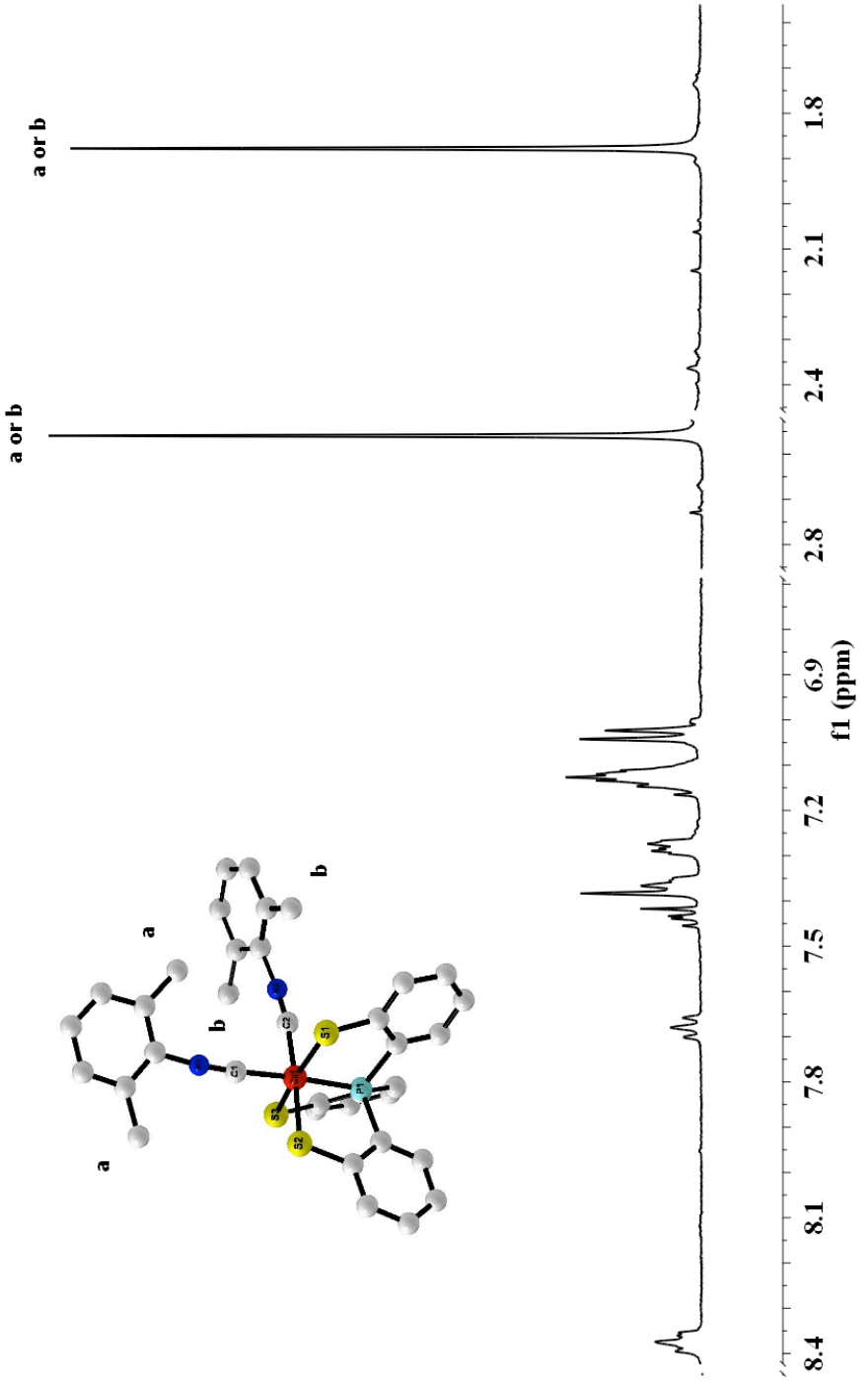

Fig 17. ^{1}H NMR spectrum $Co^{III}(PS3)(CN\text{-}Me_2Ph)_2$ (2)

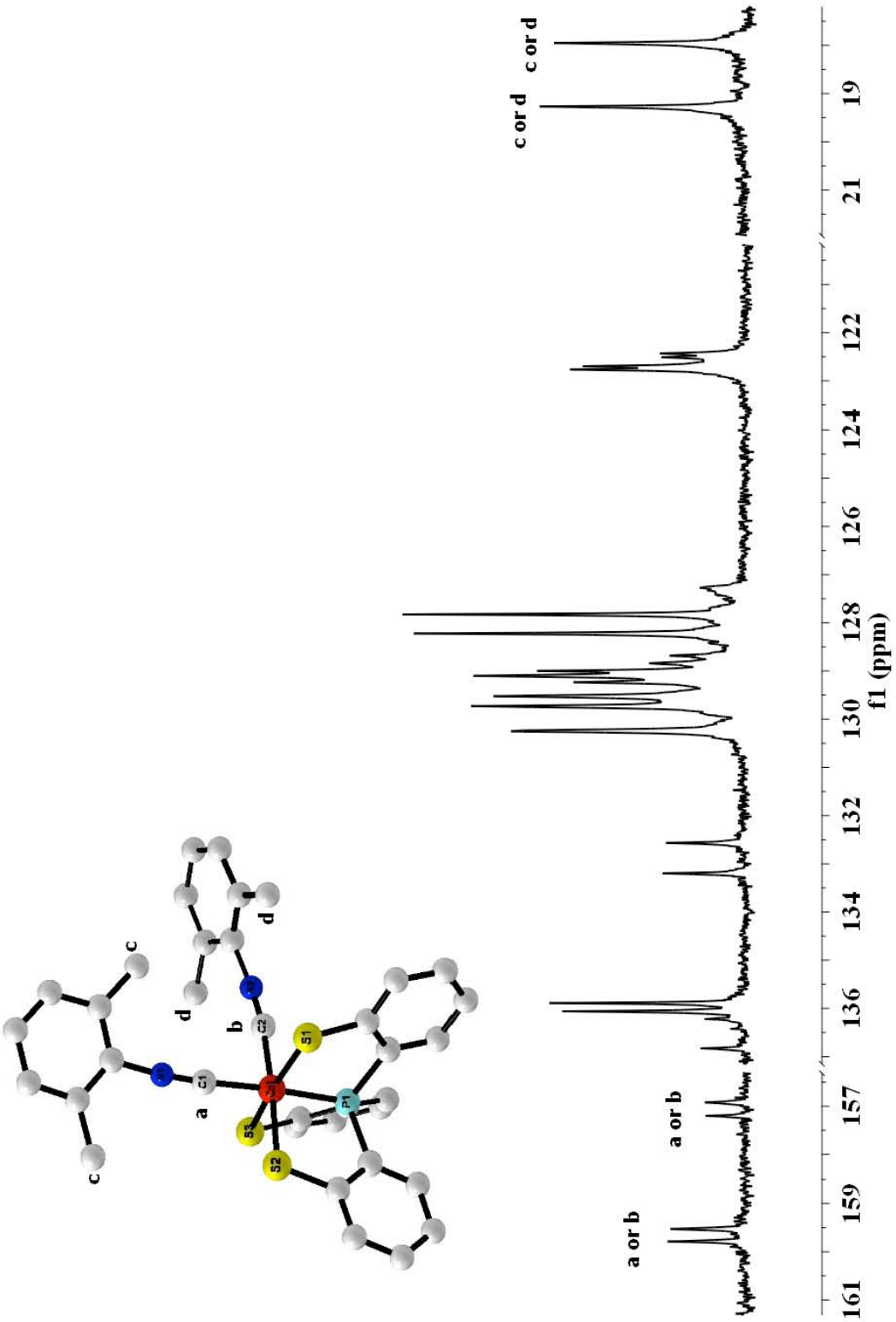

Fig 18. ^{13}C NMR spectrum $Co^{III}(PS3)(CN\text{-}Me_2Ph)_2$ (2)

Electrochemical studies revealed no reversible or irreversible peaks, so it is not shown.

The compound's UV VIS spectrum is shown below.

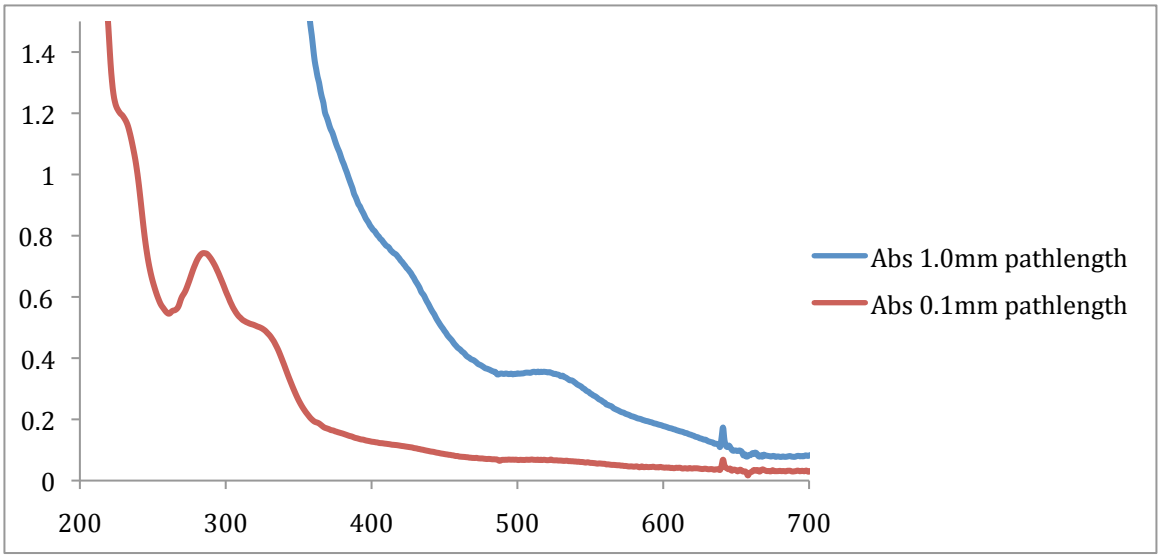

Fig 19. UV-VIS Spectrum of $Co^{III}(PS3)(CN\text{-}Me_2Ph)_2$ (2)

Chemistry of $Co^{III}(PS3)(CNC(CH_3)_3)_2$ (3)

$Co^{III}(PS3)(CNC(CH_3)_3)_2$ was synthesized by lithiating the PS3 ligand in methanol, which would then react with cobalt(II) chloride and t-butyl isocyanide to form **3**. All reagents can be added and stirred together from the beginning of the reaction, as performing the reaction in this fashion or in a stepwise manner will produce the same results. This compound is very similar to that of its iron counterpart, $Fe^{III}(PS3)(CNC(CH_3)_3)_2$, of which their similarities will be discussed later. The crystal structure reveals that this compound has an octahedral cobalt center, with three sulfurs occupying the equatorial positions of the molecule, the phosphorous in an axial position, and the tert-butyl isocyanides occupying both an axial and equatorial position.

Table 3. Bond distances and Bond Angles for $Co^{III}(PS3)(CNC(CH_3)_3)_2$ (3)

Bond Distances (Å)		**Bond Angles (Deg)**	
Co(1)-C(2)	1.850(2)	C(2)-Co(1)-C(1)	98.46(7)
Co(1)-C(1)	1.9054(19)	C(2)-Co(1)-P(1)	86.28(5)
Co(1)-P(1)	2.1327(5)	C(1)-Co(1)-P(1)	175.21(6)
Co(1)-S(1)	2.2821(6)	C(2)-Co(1)-S(1)	84.90(6)
Co(1)-S(2)	2.2823(5)	C(1)-Co(1)-S(1)	92.77(6)
Co(1)-S(3)	2.2910(5)	P(1)-Co(1)-S(1)	88.360(19)
S(1)-C(3)	1.7563(18)	C(2)-Co(1)-S(2)	174.13(6)
S(2)-C(9)	1.7508(18)	C(1)-Co(1)-S(2)	87.30(6)

S(3)-C(15)	1.7625(18)	P(1)-Co(1)-S(2)	87.976(19)
P(1)-C(10)	1.7979(17)	S(1)-Co(1)-S(2)	93.71(2)
P(1)-C(4)	1.8017(18)	C(2)-Co(1)-S(3)	88.76(6)
P(1)-C(16)	1.8034(16)	C(1)-Co(1)-S(3)	95.14(6)
C(1)-N(1)	1.147(2)	P(1)-Co(1)-S(3)	84.195(19)
C(2)-N(2)	1.150(2)	S(1)-Co(1)-S(3)	170.51(2)
		S(2)-Co(1)-S(3)	91.90(2)

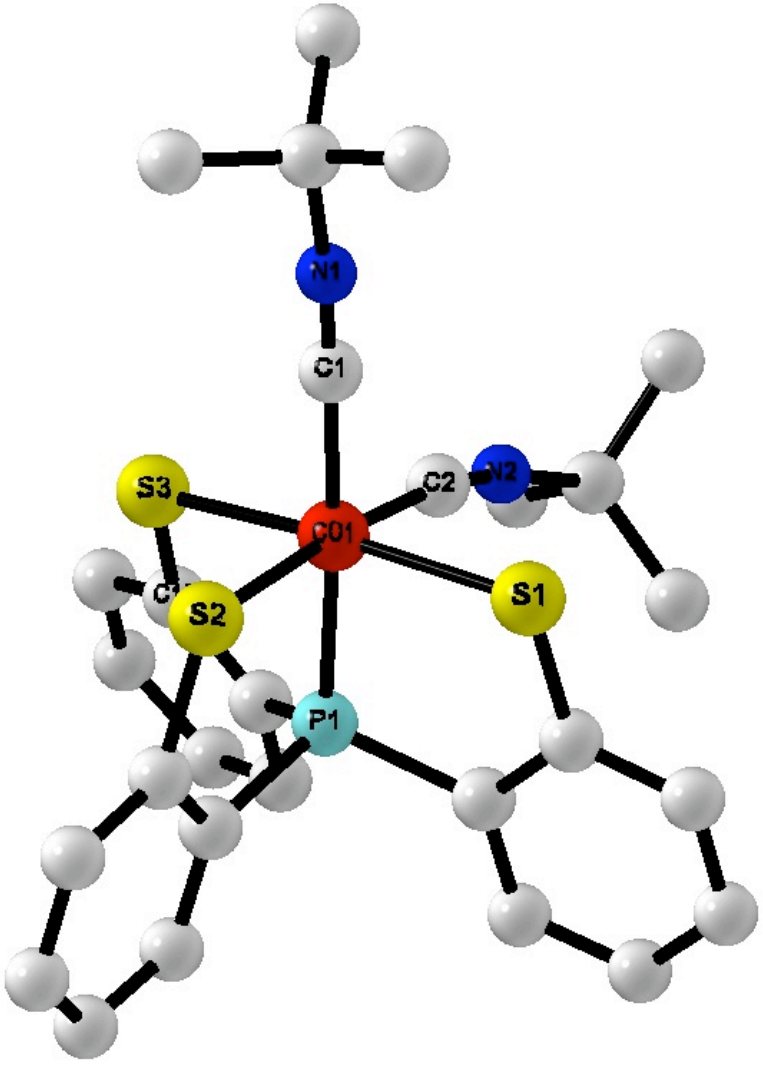

Fig 20. CHARON diagram of $Co^{III}(PS3)(CNC(CH_3)_3)_2$ (3)

The IR stretching frequencies for compound **3** in the solid state are 2162cm^{-1} and 2175cm^{-1}. The IR shows two peaks of approximately equal intensity, indicating two tert-butyl isocyanide ligands were attached to the cobalt. This was proven in the compound's crystal structure.

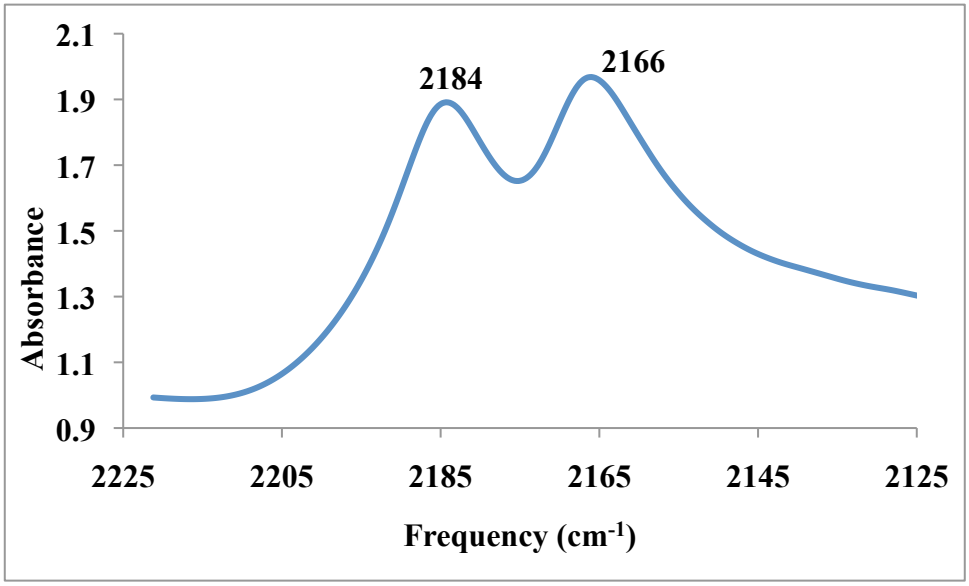

Fig 21. IR spectrum (KBr) of $Co^{III}(PS3)(CNC(CH_3)_3)_2$ (3)

The ^{1}H NMR spectrum of **3** indicates it is a diamagnetic structure, and ^{31}P NMR spectroscopy also gave a clean spectrum with only one peak appearing at 131ppm. The compound's ^{13}C NMR with assignments to some peaks is shown in figure 23. The two doublets at 159.17ppm ($^{2}J_{P\text{-}C}$ 26.3Hz) and 158.58ppm ($^{2}J_{P\text{-}C}$ 29.0Hz) are assigned to the isocyanide carbons.

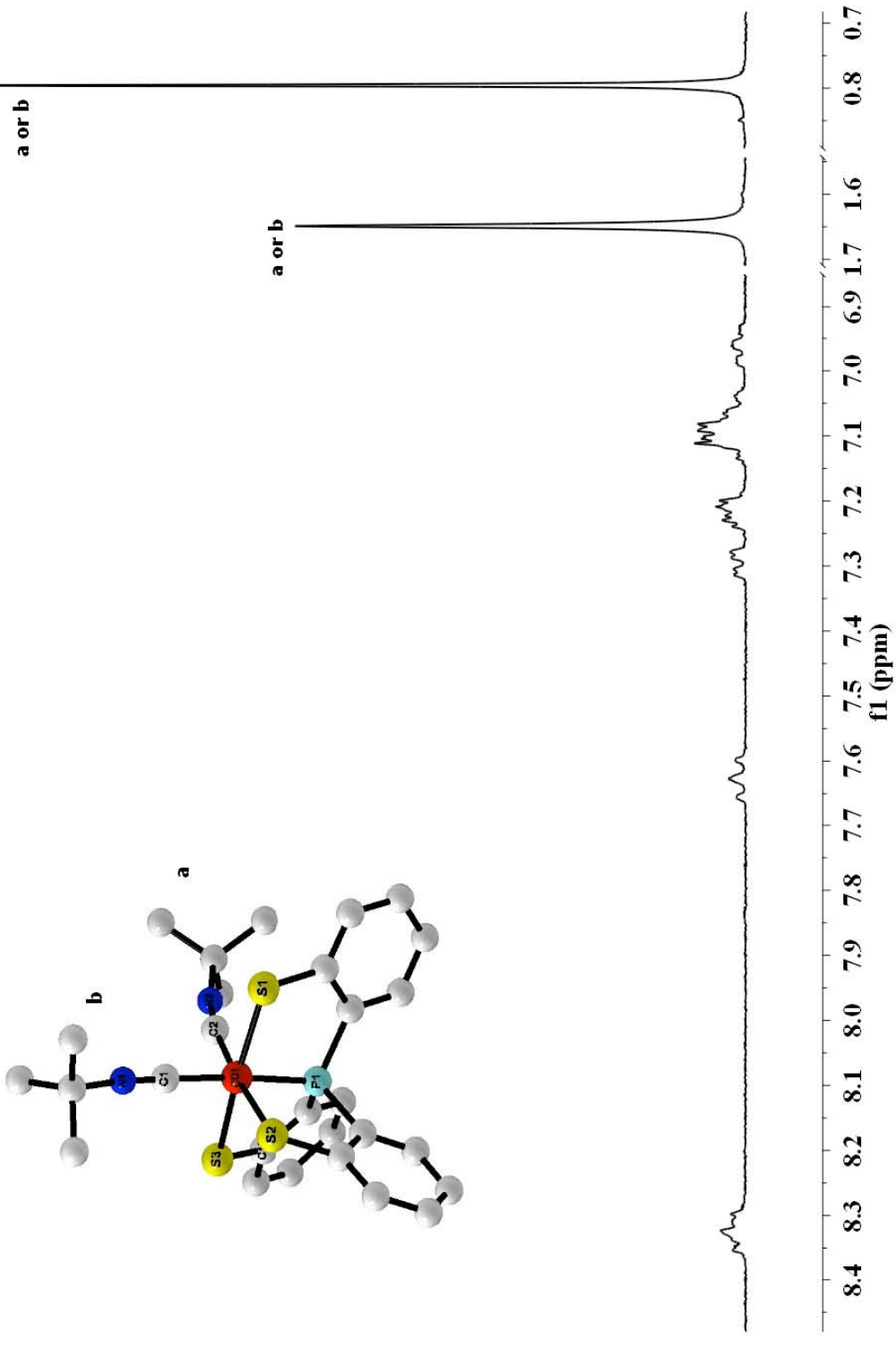

Fig 22. ^{1}H NMR spectrum of $Co^{III}(PS3)(CNC(CH_3)_3)_2$ (3)

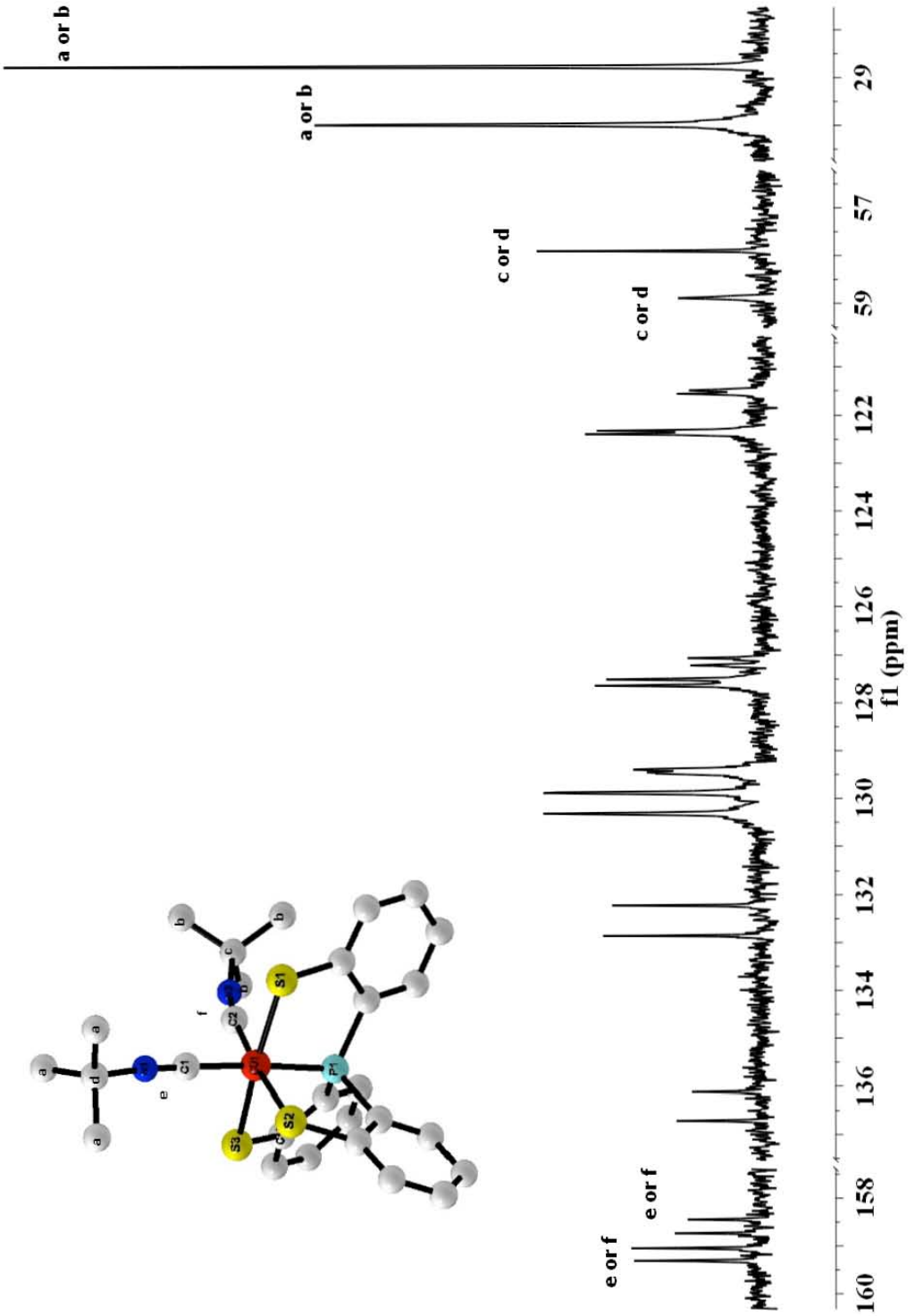

Fig 23. ^{13}C NMR spectrum of $Co^{III}(PS3)(CNC(CH_3)_3)_2$ (3)

Electrochemical studies revealed no reversible or irreversible peaks, thus were inconclusive and are not shown.

The compound's UV VIS spectrum is shown below:

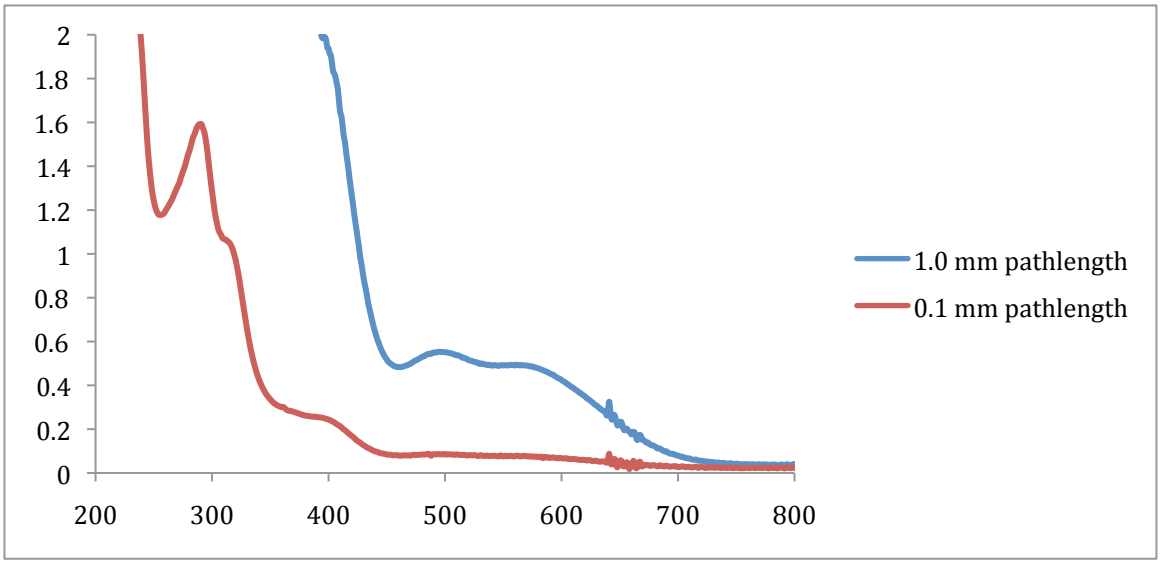

Fig 24. UV-VIS spectrum of $Co^{III}(PS3)(CNC(CH_3)_3)_2$ (3)

Chemistry of $Fe^{III}(PS3)(CN\text{-}Me_2Ph)_2$ (4)

$Fe^{III}(PS3)(CN\text{-}Me_2Ph)_2$ was synthesized by lithiating the PS3 ligand in methanol, which would then react with $FeCl_2$ and 2,6-dimethylphenyl isocyanide to form **4**. All reagents can be added and stirred together from the beginning of the reaction, as performing the reaction in this fashion or in a stepwise manner will produce the same results. The crystal structure reveals that this compound has an octahedral iron center, with three sulfurs occupying the equatorial positions of the molecule, the phosphorous in an axial position, and the dimethylphenyl isocyanides occupying both an axial and equatorial position.

Table 4. Bond Distances and Bond Angles for $Fe^{III}(PS3)(CN\text{-}Me_2Ph)_2$ (4)

Bond Distances (A)		**Bond Angles (Deg)**	
Fe(1)-C(2)	1.884(4)	C(2)-Fe(1)-C(1)	86.09(14)
Fe(1)-C(1)	1.897(4)	C(2)-Fe(1)-P(1)	95.29(10)
Fe(1)-P(1)	2.1685(9)	C(1)-Fe(1)-P(1)	177.06(11)
Fe(1)-S(2)	2.2574(10)	C(2)-Fe(1)-S(2)	174.61(11)
Fe(1)-S(3)	2.2655(10)	C(1)-Fe(1)-S(2)	89.91(10)
Fe(1)-S(1)	2.3001(10)	P(1)-Fe(1)-S(2)	88.87(4)
S(1)-C(3)	1.762(4)	C(2)-Fe(1)-S(3)	83.93(10)
S(2)-C(9)	1.768(3)	C(1)-Fe(1)-S(3)	92.04(10)
S(3)-C(15)	1.766(3)	P(1)-Fe(1)-S(3)	85.54(3)

P(1)-C(4)	1.809(3)	S(2)-Fe(1)-S(3)	99.85(4)
P(1)-C(16)	1.815(3)	C(2)-Fe(1)-S(1)	80.79(10)
P(1)-C(10)	1.813(3)	C(1)-Fe(1)-S(1)	96.83(11)
C(1)-N(1)	1.158(4)	P(1)-Fe(1)-S(1)	85.95(3)
C(2)-N(2)	1.162(4)	S(2)-Fe(1)-S(1)	96.12(4)
		S(3)-Fe(1)-S(1)	161.73(4)

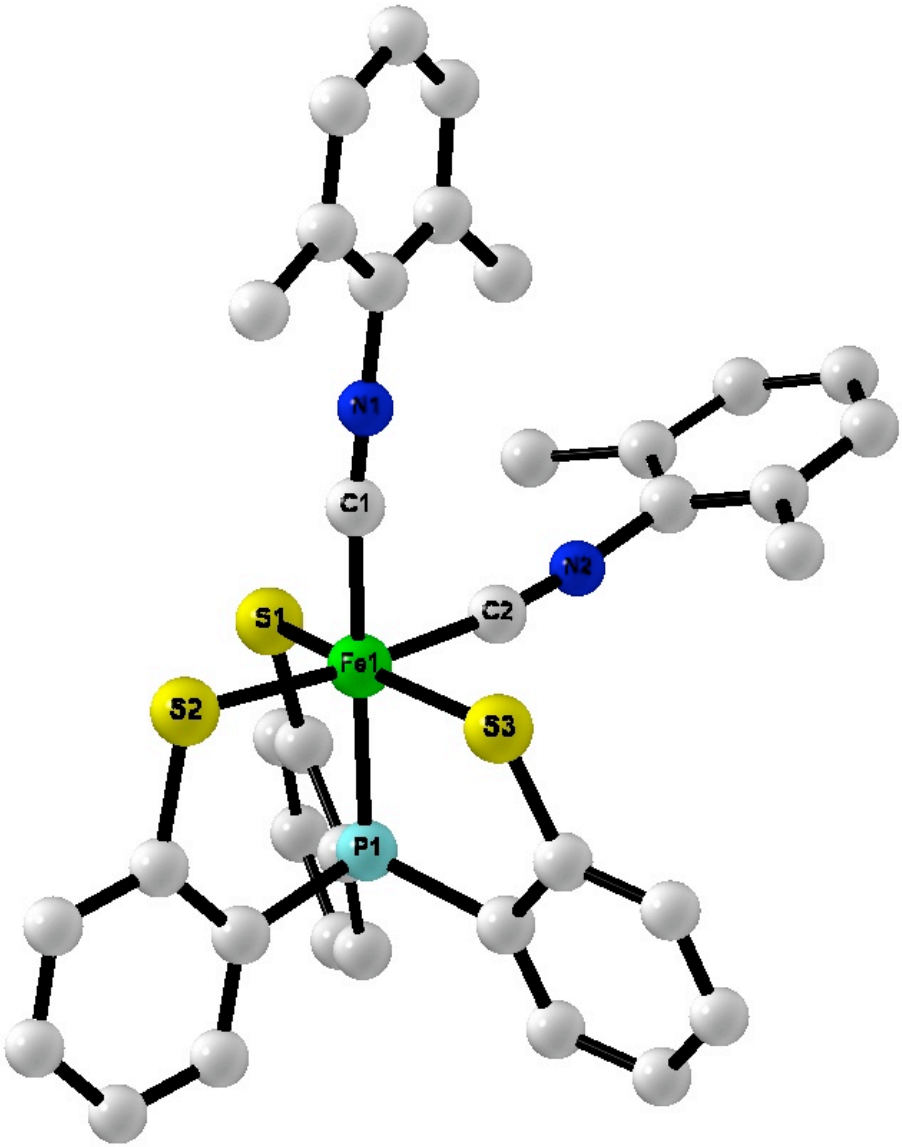

Fig 25. CHARON Diagram of $Fe^{III}(PS3)(CN\text{-}Me_2Ph)_2$ (4)

The IR stretching frequencies for compound **4** in the solid state are 2130cm^{-1} and 2154cm^{-1}. The IR shows two peaks of similar intensity, indicating two dimethylphenyl isocyanide ligands were attached to the iron. This was proven with the compound's crystal structure.

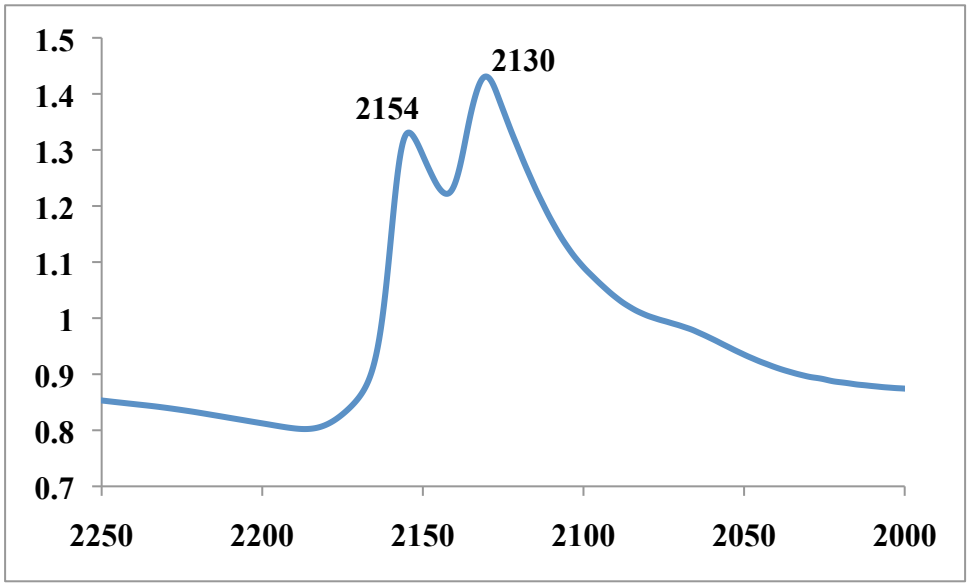

Fig 26. IR Spectrum (KBr) of $Fe^{III}(PS3)(CN\text{-}Me_2Ph)_2$ (4)

The compound is in the iron(III) oxidation state and thus was expected to be paramagnetic. After attempting ^{1}H NMR spectroscopy, it was found that the compound was indeed paramagnetic and a decent NMR spectrum could not be obtained.

However, unlike the reported cobalt compounds, this iron compound, as well as the proceeding one, gave good electrochemistry, giving a reversible reduction at -0.135V.

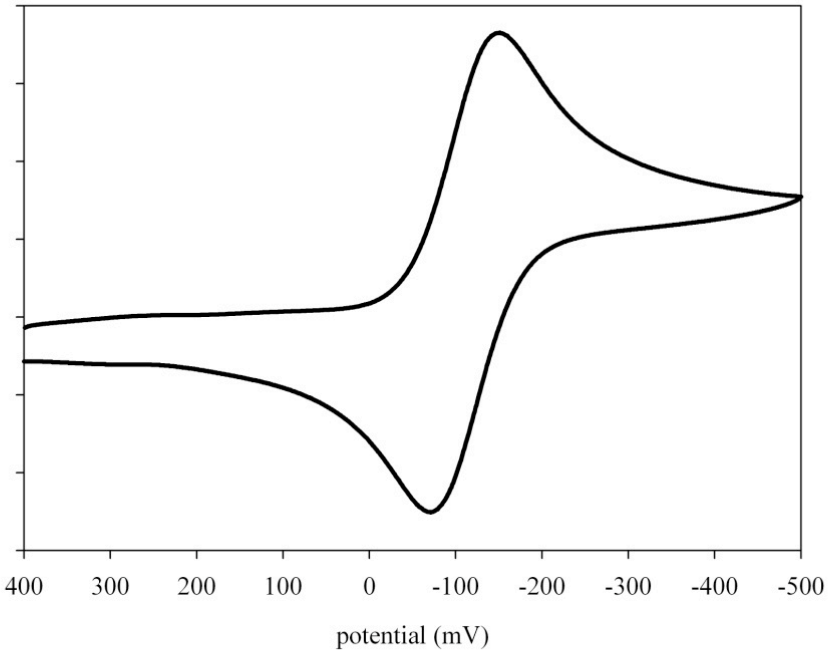

Fig 27. CV of $Fe^{III}(PS3)(CN\text{-}Me_2Ph)_2$ (4)

The compound's UV-VIS spectrum is shown below:

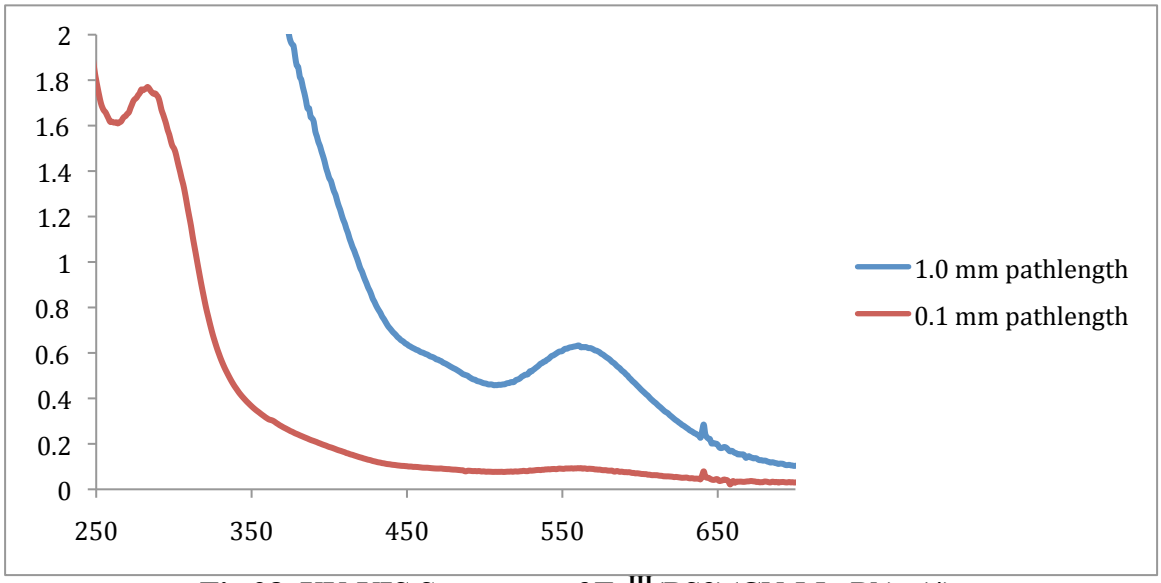

Fig 28. UV-VIS Spectrum of $Fe^{III}(PS3)(CN\text{-}Me_2Ph)_2$ (4)

Chemistry of $Fe^{III}(PS3)(CNC(CH_3)_3)_2$ (5)

$Fe^{III}(PS3)(CNC(CH_3)_3)_2$ (**5**) was synthesized by lithiating the PS3 ligand in methanol, which would then react with cobalt chloride and tert-butyl isocyanide to form **5**. All reagents can be added and stirred together from the beginning of the reaction, as performing the reaction in this fashion or in a stepwise manner will produce the same results. The crystal structure reveals that this compound has an octahedral iron center, with three sulfurs occupying the equatorial positions of the molecule, the phosphorous in an axial position, and the tert-butyl isocyanides occupying both an axial and equatorial position.

Table 5. Bond Distances and Bond Angles for $Fe^{III}(PS3)(CNC(CH_3)_3)_2$ (5)

Bond Distances (Å)		**Bond Angles (Deg)**	
Fe(1)-C(2)	1.905(2)	C(2)-Fe(1)-C(1)	98.98(8)
Fe(1)-C(1)	1.911(2)	C(2)-Fe(1)-P(1)	85.41(6)
Fe(1)-P(1)	2.1559(5)	C(1)-Fe(1)-P(1)	175.61(6)
Fe(1)-S(3)	2.2644(5)	C(2)-Fe(1)-S(3)	85.32(6)
Fe(1)-S(1)	2.2725(6)	C(1)-Fe(1)-S(3)	94.89(6)
Fe(1)-S(2)	2.2821(6)	P(1)-Fe(1)-S(3)	85.27(2)
S(1)-C(3)	1.7616(18)	C(2)-Fe(1)-S(1)	82.67(6)
S(2)-C(9)	1.7618(19)	C(1)-Fe(1)-S(1)	92.80(6)
S(3)-C(15)	1.7667(18)	P(1)-Fe(1)-S(1)	87.89(2)

P(1)-C(10)	1.7966(19)	S(3)-Fe(1)-S(1)	166.61(2)
P(1)-C(4)	1.8079(18)	C(2)-Fe(1)-S(2)	172.71(6)
P(1)-C(16)	1.8110(17)	C(1)-Fe(1)-S(2)	88.23(6)
C(1)-N(1)	1.156(2)	P(1)-Fe(1)-S(2)	87.38(2)
C(2)-N(2)	1.151(2)	S(3)-Fe(1)-S(2)	95.16(2)
		S(1)-Fe(1)-S(2)	96.00(2)

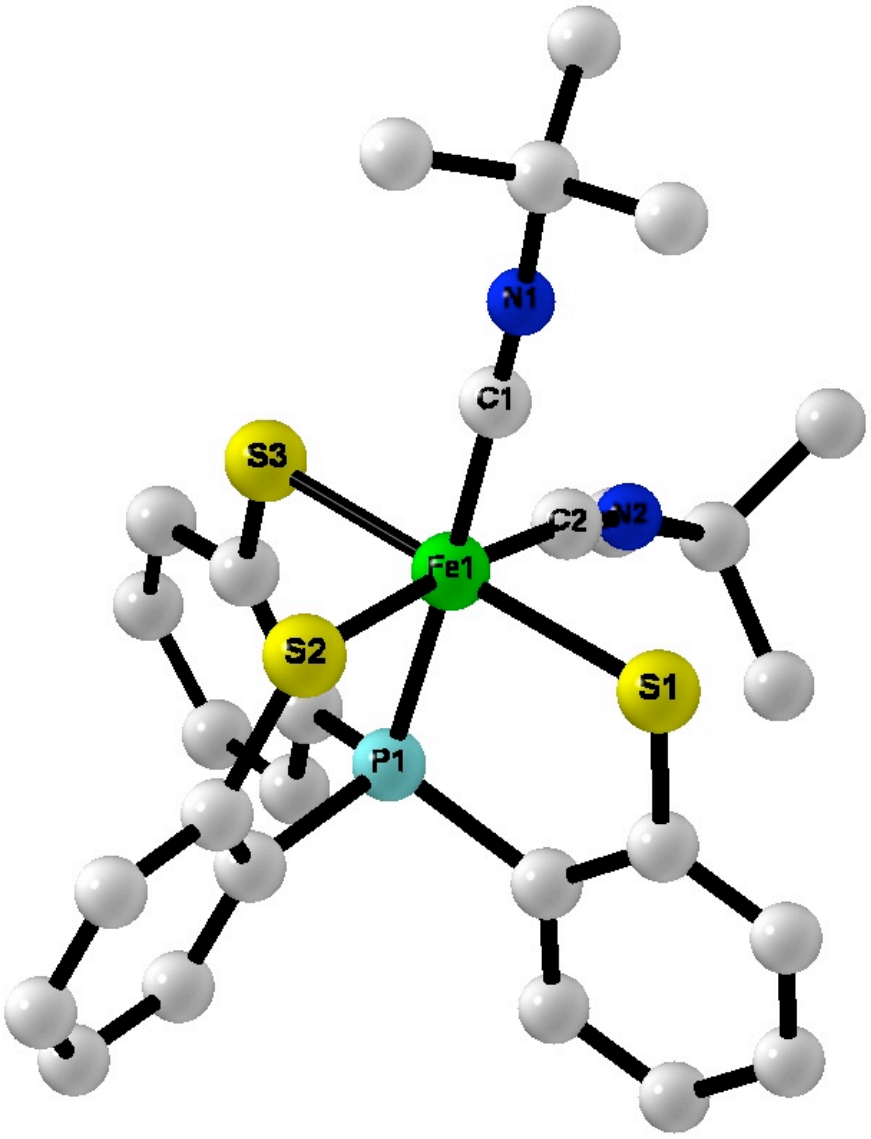

Fig 29. CHARON Diagram of $Fe^{III}(PS3)(CNC(CH_3)_3)_2$ (5)

The IR stretching frequencies for compound **5** in the solid state are 2142cm^{-1} and 2158cm^{-1}. The IR shows two peaks of approximately equal intensity, indicating two *tert*-butyl isocyanide ligands were attached to the iron. This was proven with the compound's crystal structure.

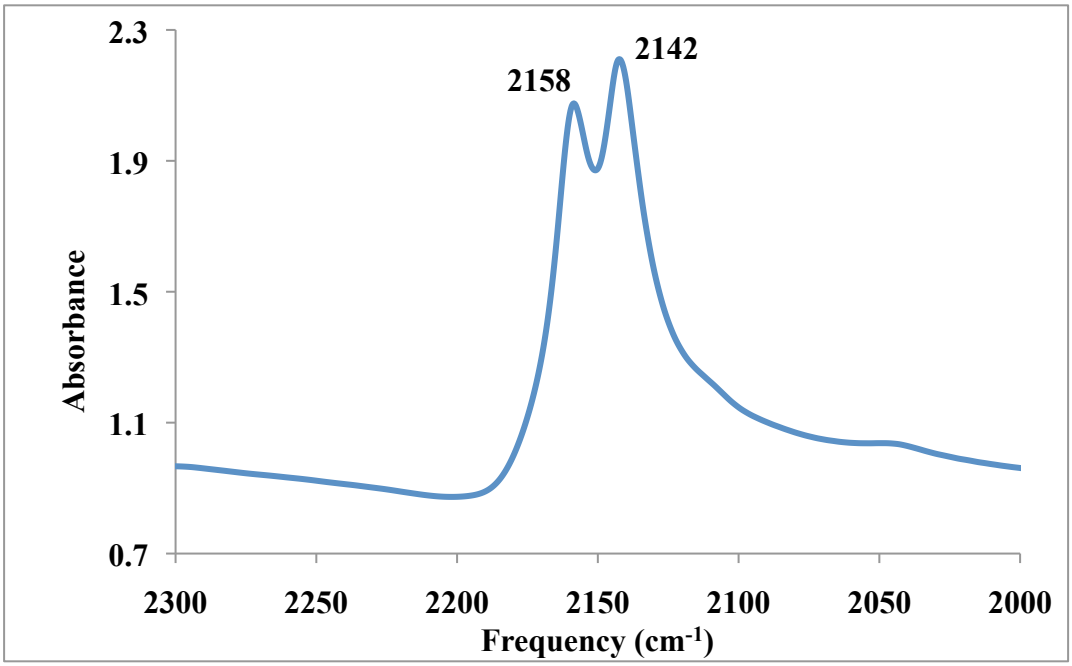

Fig 30. IR Spectrum (KBr) of $Fe^{III}(PS3)(CNC(CH_3)_3)_2$ (5)

The compound is in the iron(III) oxidation state and thus was expected to be paramagnetic. After attempting NMR spectroscopy, it was found that the compound was indeed paramagnetic and a decent NMR spectrum could not be obtained.

However, unlike the cobalt compounds, this iron compound, as well as the preceding one, gave good electrochemistry, showing a reversible reduction at -0.260V.

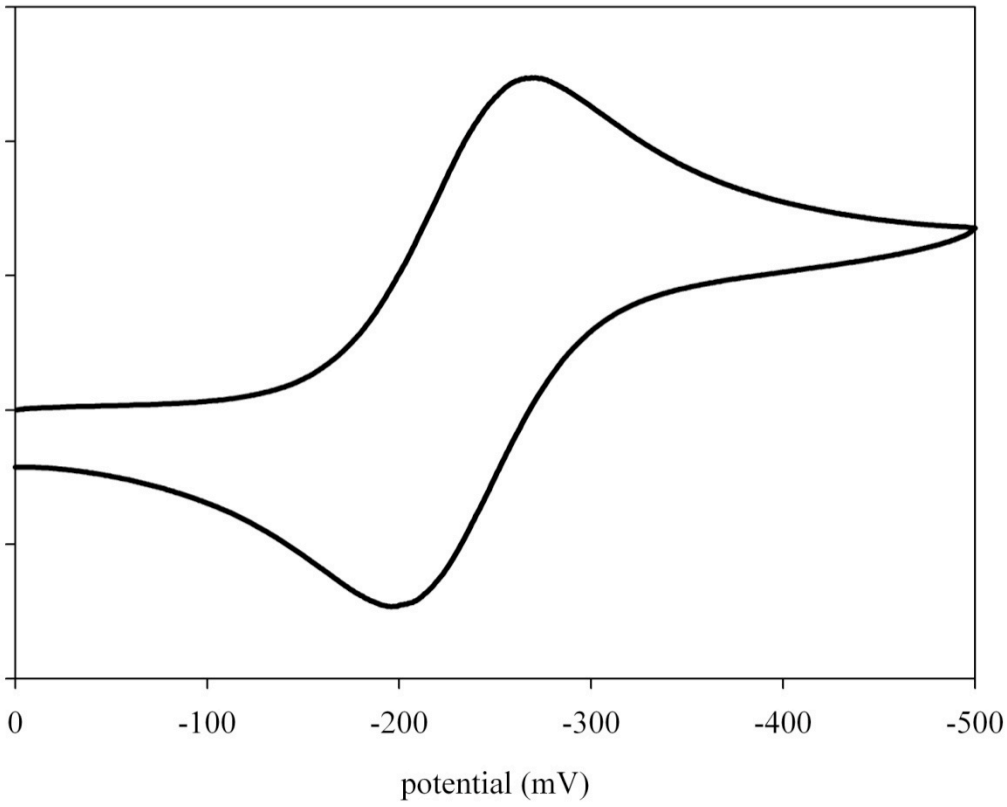

Fig 31. Cyclic Voltammogram of $Fe^{III}(PS3)(CNC(CH_3)_3)_2$ (5)

The compound also gave a UV VIS spectrum, and its extinction coefficients of the peaks are shown below. This spectrum will be compared to the ones found for the other compounds later on.

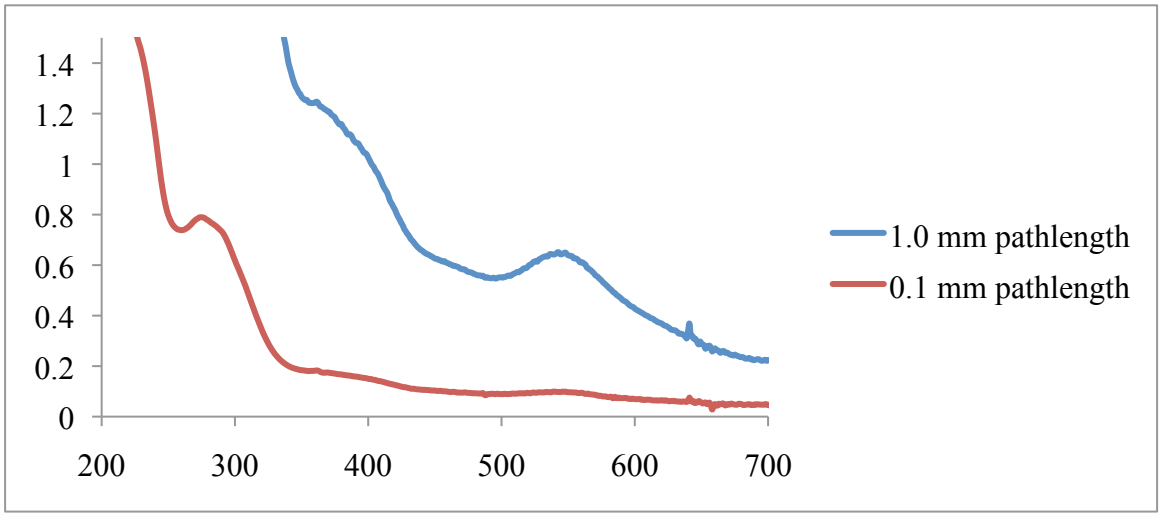

Fig 32. UV-VIS spectrum of $Fe^{III}(PS3)(CNC(CH_3)_3)_2$ (5)

Structural Comparisons

The metal-ligand bond distances are compared in Tables 6 and 7. Also included are the bond distances from the previously studied $[Fe^{III}(PS3)(CN)_2]^{2-}$ complex. The general observation is that the analogous distances are all remarkably similar. Among the isocyanide complexes, the Co-P and the Co-C (trans to S) are slightly shorter than the corresponding distances in the Fe compounds. The M_{ave}-S distances for the Co compounds are very slightly longer. The differences are only statistically significant because the structures were collected on the new Oxford diffractometer. The same small differences in the bond distances are found in the comparison of the Co and Fe CN complexes.

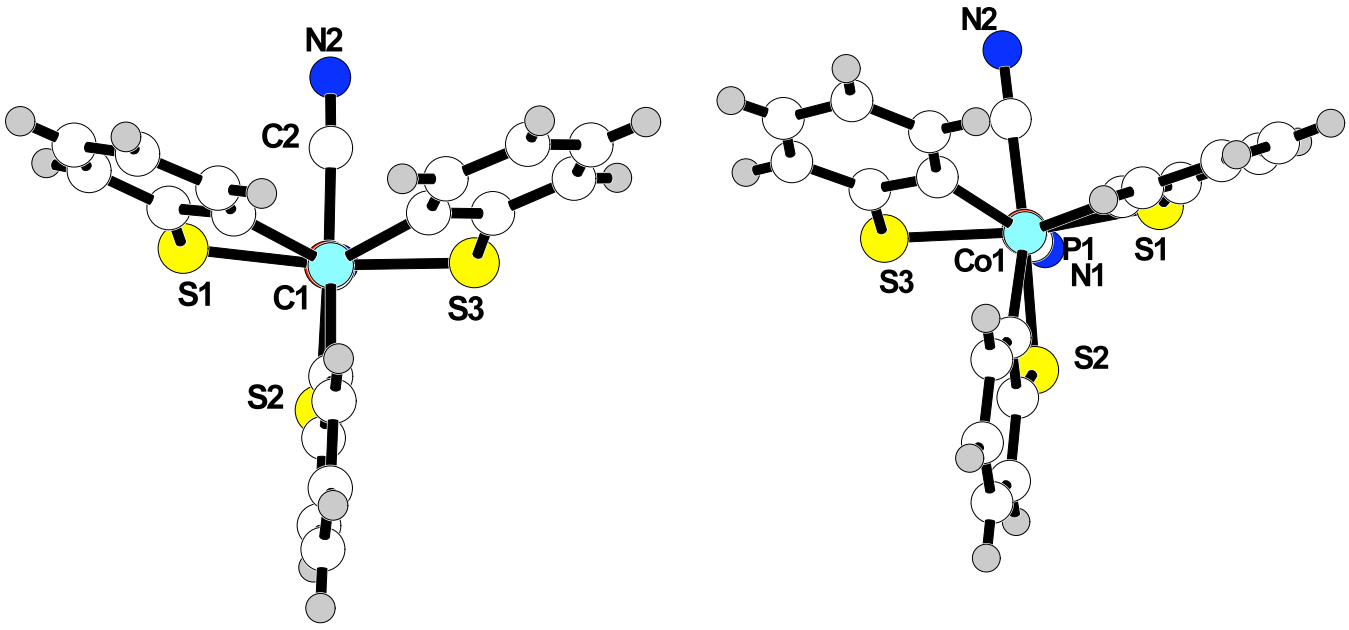

Fig 33 and 34. $Co^{III}(PS3)(CN\text{-}Me_2Ph)_2$ with the phenyl rings removed; $[Co^{III}(PS3)(CN)_2]^{2-}$

Two structural features deserve comment. A view down the P-Co bond in the $Co^{III}(PS3)(CN\text{-}Me_2Ph)_2$. Figure 33 shows that the structure has a non-crystallographic mirror plane. Similar structural diagrams are found for the other compounds with the exception of the $[Co^{III}(PS3)(CN)_2]^{2-}$ compound which is distorted away from Cs symmetry. The distortions in binding of the chelate ring to Co is manifested in the significantly difference in Co-S distances of the trans S ligands which are 2.2652(8) Å and 2.3241(8)Å. The conformational distortion of the binding of the PS3 ligand to the metal is likely due to packing forces in the crystal. The uncoordinated PS3 ligand has trigonal symmetry. When it binds to an octahedral metal center it has to adopt confirmations which no longer have the C_3 axis. The NMR spectra of all the Co complexes are consistent with Cs symmetry in solution.

The second structural feature is the large difference in C-M-C angles in the compounds with the different isonitrile ligands. C1-M-C2 angles are 86.66(8)º (Co) and 86.09(14)º (Fe) in the isomorphous complexes with the 2,6-dimethylphenyl isocyanide and 98.46(7)º (Co) and 98.98(8)º (Fe) in the isomorphous Co and Fe complexes with the t-butyl isocyanide ligands. The increase of angle in the t-butyl isocyanide compounds does not appear to caused by the steric interaction between the isocyanide ligands.

Table 6. Comparisons of Bond Distances for isocyanide compounds

$Co^{III}(PS3)(CNC(CH_3)_3)_2$ (3)		**$Fe^{III}(PS3)(CNC(CH_3)_3)_2$ (5)**		**$Co^{III}(PS3)(CN\text{-}Me_2Ph)_2$ (2)**		**$Fe^{III}(PS3)(CN\text{-}Me_2Ph)_2$ (4)**	
Co(1)-C(2)	1.850(2)	Fe(1)-C(2)	1.905(2)	Co(1)-C(2)	1.838(2)	Fe(1)-C(2)	1.884(4)
Co(1)-C(1)	1.9054(19)	Fe(1)-C(1)	1.911(2)	Co(1)-C(1)	1.891(2)	Fe(1)-C(1)	1.897(4)
Co(1)-P(1)	2.1327(5)	Fe(1)-P(1)	2.1559(5)	Co(1)-P(1)	2.1402(5)	Fe(1)-P(1)	2.1685(9)
Co(1)-S(1)	2.2821(6)	Fe(1)-S(1)	2.2725(6)	Co(1)-S(2)	2.2708(6)	Fe(1)-S(2)	2.2574(10)
Co(1)-S(2)	2.2823(5)	Fe(1)-S(2)	2.2821(6)	Co(1)-S(3)	2.2835(6)	Fe(1)-S(3)	2.2655(10)
Co(1)-S(3)	2.2910(5)	Fe(1)-S(3)	2.2644(5)	Co(1)-S(1)	2.2901(6)	Fe(1)-S(1)	2.3001(10)
$Co\text{-}S_{ave}$	2.285(5)	$Fe\text{-}S_{ave}$	2.273(8)	$Co\text{-}S_{ave}$	2.281(9)	$Fe\text{-}S_{ave}$	2.274(22)
C(1)-N(1)	1.147(2)	C(1)-N(1)	1.156(2)	C(1)-N(1)	1.145(2)	C(1)-N(1)	1.158(4)
C(2)-N(2)	1.150(2)	C(2)-N(2)	1.151(2)	C(2)-N(2)	1.147(2)	C(2)-N(2)	1.162(4)

Table 7. Comparisons of Bond Distances for Cobalt and Iron cyanide compounds

$[Me_3NBz]_2[Co^{III}(PS3)(CN)_2]$		$[Me_3NBz]_2[Fe^{III}(PS3)(CN)_2]$	
Co(1)-C(2)	1.8769(17)	Fe(1)-C(2)	1.968(13)
Co(1)-C(1)	1.9302(18)	Fe(1)-C(1)	2.021(16)
Co(1)-P(1)	2.1167(8)	Fe(1)-P(1)	2.127(4)
Co(1)-S(1)	2.2652(8)	Fe(1)-S(1)	2.287(4)
Co(1)-S(2)	2.2776(10)	Fe(1)-S(2)	2.282(6)
Co(1)-S(3)	2.3241(8)	Fe(1)-S(3)	2.260(4)
$Co\text{-}S_{ave}$	2.289(31)	$Fe\text{-}S_{ave}$	2.276(14)
C(1)-N(1)	1.157(2)	C(1)-N(1)	1.147(16)
C(2)-N(2)	1.1595(19)	C(2)-N(2)	1.152(14)

Comparison of Spectroscopic Properties

The IR, and Electronic spectra were measured for all the new compounds. NMR spectra were measured for the diamagnetic Co(III) compounds. Due to the paramagnetism of the Fe(III) complexes, no NMR spectra could be obtained. The NMR spectra are consistent with the X-ray crystal structures. The compounds are all intensely colored with strong absorptions in the visible region. The intensity of the bands is such that they are likely due to ligand to metal charge transfer transitions. In the absence of high level quantum mechanical calculations, it is not possible to further interpret the spectra.

All the compounds show two peaks of nearly the same intensity in their IR spectra for the C-N stretches of the formally C-N triple bonds (table 8). The spectra are consistent with the cis arrangement of the ligands. The cobalt compounds all consistently appear at higher wavenumbers than their iron counterparts. Also, for both the Fe and Co complexes, there is a trend that the t-butyl ligands appear at the highest wavenumbers, the dimethylphenyl ligands come in the middle, and the cyanide ligand appear at the lowest wavenumbers.

Table 8. Comparison of IR spectra

$[Co^{III}(PS3)(CN)_2]^{2-}$	**2112**	**2089**
$[Fe^{III}(PS3)(CN)_2]^{2-}$	**2084**	**2076**
$Co^{III}(PS3)(CN\text{-}Me_2Ph)_2$ (2)	**2175**	**2162**
$Fe^{III}(PS3)(CN\text{-}Me_2Ph)_2$ (4)	**2154**	**2130**
$Co^{III}(PS3)(CNC(CH_3)_3)_2$ (3)	**2184**	**2166**
$Fe^{III}(PS3)(CNC(CH_3)_3)_2$ (5)	**2158**	**2142**

Summary, Conclusion and Future Work

Our initial investigation of cobalt complexes with the PS3 ligand resulted in the characterization of three $[(PS3)Co^{III}L_2]^{n-}$ complexes where L = CN^- and where L is the isocyanide ligands : 2,6-dimethylphenylisocyanide and *t*-butylisocyanide. The CN^- complex is structurally similar to the previously characterized Fe analog, $[(PS3)Fe^{III}(CN)_2]^{2-}$. No isocyanide complexes of iron with the PS3 ligand had been previously characterized. We synthesized and characterized a set of Fe isocyanide complexes $[(PS3)Fe^{III}(L_2)]$ with the same two isocyanide ligands. The complexes were isomorphous and isostructural with the Co complexes. The three successfully characterized cobalt complexes were octahedral in the +3 oxidation state. NMR studies confirmed that the compounds are diamagnetic, with low spin d^6 electronic configurations. The ^1H, ^{13}C and ^{31}P NMR studies indicate that the cobalt complexes have the same structure in solution that they have in the solid state. Since low spin octahedral d^6 complexes have the highest possible ligand field stabilization energy, it is not surprising that octahedral $[(PS3)Co^{III}(L_2)]$ complexes were isolated. The new iron isocyanide complexes and the previously characterized CN- complex are low spin d^5.

Although the three cobalt(III) complexes are isostructural with their Fe(III) complexes, they differ considerably in their electrochemical behavior. The Fe(III) complexes show reversible 1 e- reduction waves indicating the Fe(II) analogs should be stable. The Co complexes show no reversible reductions indicating that a Co(II) complex is much less stable with respect to oxidation than is the Fe(II) complex. The electrochemical behavior is reflected in our observations during the synthetic reactions which resulted in the isolation of the Fe(III) and Co(III) complexes. All the complexes

were synthesized by reacting Li_3(PS3) with $CoCl_2$ or $FeCl_2$ in MeOH. Based on the IR spectroscopy, we have generated the Fe(II) complexes in solution in our synthesis. The IR spectra of the reaction mixture shows two peaks, which is consistent with the generation of $[(PS3)Fe^{II}L_2]^{1-}$ complexes. The energy of the isocyanide stretching frequencies are lower in energy than those found in the characterized Fe(III) complexes; this is consistent with more backbonding from the metal to the isocyanide ligands in the Fe(II) complex. Upon the addition of air, the isocyanide stretching frequencies of the Fe(II) complex are replaced by those of the Fe(III) product. On the other hand, the reaction of $CoCl_2$ with Li_3(PS3) in MeOH results in the direct production of the Co(III) complexes without the addition of air or other additional oxidizing agent. The oxidation from Co(II) to Co(III) is believed to occur by the reduction of H^+ from the MeOH to yield H_2. No attempt was made to detect and measure hydrogen in this system; but reduction of protons to H_2 has been previously shown to occur in reactions of Co(II) with the related Li_2PS2 ligand. Systems, which produce H_2, are on significant interest as models for the hydrogenase enzymes.

Two synthetic approaches were pursued to isolate a Co(II) complex. With the assumption that MeOH was the source of oxidizing agent, Li3(PS3) was reacted with $CoCl_2$ in the non-protic solvent CH_3CN. In a second strategy , CO was used as a possible ligand to stabilize a Co(II) complexes. In neither case was it possible to isolate a Co(II) complex.

The isolation of an octahedral (PS3)ML_2 complex with a particular L ligand does not preclude the possibility that five coordinate trigonal bipyramidal (PS3)ML complexes could be obtained with the same Ligand. In previous work, both 5 and 6 coordinate

complexes with the same L ligand have been obtained: $[(PS3)Fe^{II}(CO)]^{1-}$ and $[(PS3)Fe^{II}(CO)_2]^{1}$ and $[(PS3)Fe^{III}(CN)]^{1-}$ and $[(PS3)Fe^{III}(CN)_2]^{2-}$.

It would be useful to obtain an isostructural series of Fe, Co and Ni complexes with the same oxidation. The characterization of $[(PS3)Co^{II}(CO)]^{1-}$ would produce such a series. Since Ni(II) and Ni(III) complexes with the (PS3)Ni(CN-2,5-Me_2Ph) are known, the preparation of M(II) or M(III) complexes of Co and Fe would generate an additional series. It would be possible to directly compare the effect of changing the Metal on trends in redox potentials, spectroscopic properties and reactivity.

However, we have not been able to successfully isolate and crystallize these complexes. While these compounds were very similar to one another, they did show some differences among the types of ligands used as well as with the metal centers. Also, the trend that the ligands of the cobalt compounds were always at a higher wavenumber than its iron compounds held true. Overall, the compounds were very similar, but their subtle differences are what makes them interesting to compare and to help build on this work. One of the more lucrative applications of these compounds comes with the electrochemistry of the iron compounds, which show that iron(II) versions are electrochemically possible, and may lead to applications in an ability to reduce protons into molecular hydrogen.

References

1. Vincent, K. A.; Parkin, A.; Armstrong, F. A., *Chem. Rev.* **2007,** *107*, 4366-4413.

2. Vignais, P. M.; Billoud, B., *Chem. Rev.* **2007,** *107*, 4206-4272.

3. Kubas, G. J., *Chem. Rev.* **2007,** *107*, 4152-4205.

4. De Lacey, A. L.; Fernandez, V. M.; Rousset, M.; Cammack, R., *Chem. Rev.* **2007,** *107*, 4304-4330.

5. Parkin, A.; Cavazza, C.; Fontecilla-Camps, J. C.; Armstrong, F. A., *J. Am. Chem. Soc.* **2006,** *128*, 16808-16815.

6. Hambourger, M.; Moore, G. F.; Kramer, D. M.; Gust, D.; Moore, A. L.; Moore, T. A., *Chem. Soc. Rev.* **2009,** *38*, 25-35.

7. Liu, T. B.; Darensbourg, M. Y., *J. Am. Chem. Soc.* **2007,** *129*, 7008-+.

8. Thomas, C. M.; Liu, T. B.; Hall, M. B.; Darensbourg, M. Y., *Inorg. Chem.* **2008,** *47*, 7009-7024.

9. Barton, B. E.; Rauchfuss, T. B., *Inorg. Chem.* **2008,** *47*, 2261-2263.

10. Nguyen, D. H.; Hsu, H.-F.; Millar, M.; Koch, S. A.; Achim, C.; Bominaar, E.; Münck, E., *J. Am. Chem. Soc.* **1996,** *118*, 8963-8964.

11. Nguyen, D. H. Synthesis and Characterization of Nickel-Thiolate Complexes as a Model of the Active SIte of [Ni-Fe] Hydrogenanase Enzymes. SUNY Stony Brook, Stony Brook, 1997.

12. Conradie, J.; Quarless, D. A.; Hsu, H. F.; Harrop, T. C.; Lippard, S. J.; Koch, S. A.; Ghosh, A., *J. Am. Chem. Soc.* **2007,** *129*, 10446-10456.

13. Hsu, H.-F. Synthesis and Characterization of Iron Complexes of *Tris* Thiolate Phosphine Tripod Ligands as Models of the FeS_3 Centers of Nitrogenase and $[Fe(CO)(CN)_2]$ Center of Hydrogenase. SUNY Stony Brook, Stony Brook, 1997.

14. Hsu, H.-F.; Koch, S. A.; Popescu, C. V.; Münck, E., *J. Am. Chem. Soc.* **1997,** *119*, 8371-8372.

15. Jiang, J. Studies of Fundamental [Fe(CN)$_{(6-x)}$ Compounds and Their Relation to Ni/Fe and Fe-only Hydrogenase Enzymes. SUNY Stony Brook, Stony Brook, 2002.

16. Acunzo, A. A. Synthesis and Characterization of Iron-Cyanide Complexes as Models for the Active SIte of Hydrogenase Enzymes. SUNY Stony Brook, Stony Brook, 1999.

17. Nguyen, D. H.; Hsu, H.-F.; Millar, M.; Koch, S. A.; Achim, C.; Bominaar, E.; Muenck, E., *J. Am. Chem. Soc.* **1996,** *118*, 8963-8964.

Appendix

Table A-1. Crystallographic Data for $[Me_3NBz]_2[Co^{III}(PS3)(CN)_2]$ (1)

Complex	**$[Me_3NBz]_2[Co^{III}(PS3)(CN)_2]$**	
Empirical formula	$C_{40}\ H_{44}\ Co\ N_4\ P\ S_3$	
Formula weight	766.87	
Crystal Color	red	
Temperature	100(2) K	
Wavelength	0.71069 Å	
Crystal system	triclinic	
Space group	P1bar (#2)	
Unit cell dimensions	a = 9.452(5) Å	α= 95.719(5)°
	b = 13.474(5) Å	β= 93.666(5)°
	c = 15.131(5) Å	γ = 98.801(5)°
Volume	1888.7(14) $Å^3$	
Z	2	
Density (calculated)	1.348 Mg/m^3	
Absorption coefficient	0.697 mm^{-1}	
F(000)	804	
Crystal size	0.5 x 0.4 x 0.2 mm^3	
Theta range for data collection	2.97 to 33.00°.	
Index ranges	-14<=h<=13, -16<=k<=20, -23<=l<=22	
Reflections collected	22731	
Independent reflections	12553 [R(int) = 0.0343]	
Completeness to theta = 33.00°	88.1 %	
Refinement method	Full-matrix least-squares on F^2	
Data / restraints / parameters	12553 / 0 / 442	
Goodness-of-fit on F^2	0.927	
Final R indices [I>2sigma(I)]	R1 = 0.0374, wR2 = 0.0823	
R indices (all data)	R1 = 0.0632, wR2 = 0.0865	
Largest diff. peak and hole	0.689 and -0.703 e.$Å^{-3}$	

Table A-2. Crystallographic Data for $Co^{III}(PS3)(CN\text{-}Me_2Ph)_2$ (2)

Complex	**$Co^{III}(PS3)(CN\text{-}Me_2Ph)_2$**	
Empirical formula	$C_{36}\ H_{30}\ Co\ N_2\ P\ S_3$	
Formula weight	676.70	
Crystal Color	Green	
Temperature	293(2) K	
Wavelength	0.71073 Å	
Crystal system	Monoclinic	
Space group	$P2_1$	
Unit cell dimensions	a = 10.5211(3) Å	α= 90°
	b = 14.1155(4) Å	β= 110.388(3)°
	c = 11.5391(3) Å	γ = 90°
Volume	1606.32(8) $Å^3$	
Z	2	
Density (calculated)	1.399 Mg/m^3	
Absorption coefficient	0.808 mm^{-1}	
F(000)	700	
Crystal size	0.4 x 0.3 x 0.2 mm^3	
Theta range for data collection	3.24 to 35.09°.	
Index ranges	-16<=h<=10, -21<=k<=17, -18<=l<=18	
Reflections collected	14031	
Independent reflections	10006 [R(int) = 0.0175]	
Completeness to theta = 35.09°	92.1 %	
Absorption correction	Semi-empirical from equivalents	
Max. and min. transmission	1 and 0.94352	
Refinement method	Full-matrix least-squares on F^2	
Data / restraints / parameters	10006 / 1 / 388	
Goodness-of-fit on F^2	0.856	
Final R indices [I>2sigma(I)]	R1 = 0.0326, wR2 = 0.0640	
R indices (all data)	R1 = 0.0590, wR2 = 0.0690	
Absolute structure parameter	0.011(8)	
Largest diff. peak and hole	0.274 and -0.254 e.$Å^{-3}$	

Table A-3. Crystallographic Data for $Co^{III}(PS3)(CNC(CH_3)_3)_2$ (3)

Complex	**$Co^{III}(PS3)(CNC(CH_3)_3)_2$**	
Empirical formula	$C_{28}\ H_{30}\ Co_1\ N_2\ P_1\ S_3$	
Formula weight	580.50	
Crystal Color	Dark Purple	
Temperature	293(2) K	
Wavelength	0.71073 Å	
Crystal system	monoclinic	
Space group	$P2_1/n$	
Unit cell dimensions	a = 11.0478(2) Å	α= 90°
	b = 11.8474(2) Å	β= 102.603(2)°
	c = 22.0103(4) Å	γ = 90°
Volume	2811.46(9) $Å^3$	
Z	4	
Density (calculated)	1.372 Mg/m^3	
Absorption coefficient	0.910 mm^{-1}	
F(000)	1208	
Crystal size	0.4 x 0.3 x 0.1 mm^3	
Theta range for data collection	2.86 to 29.51°.	
Index ranges	-15<=h<=7, -15<=k<=14, -30<=l<=30	
Reflections collected	15198	
Independent reflections	6711 [R(int) = 0.0339]	
Completeness to theta = 29.51°	85.5 %	
Absorption correction	None	
Refinement method	Full-matrix least-squares on F^2	
Data / restraints / parameters	6711 / 0 / 316	
Goodness-of-fit on F^2	0.814	
Final R indices [I>2sigma(I)]	R1 = 0.0309, wR2 = 0.0556	
R indices (all data)	R1 = 0.0654, wR2 = 0.0591	
Largest diff. peak and hole	0.329 and -0.283 $e.Å^{-3}$	

Table A-4. Crystallographic Data for $Fe^{III}(PS3)(CN\text{-}Me_2Ph)_2$ (4)

Complex	**$Fe^{III}(PS3)(CN\text{-}Me_2Ph)_2$**	
Empirical formula	$C_{36}\ H_{30}\ Fe\ N_2\ P\ S_3$	
Formula weight	673.62	
Crystal Color	Dark Purple	
Temperature	100 K	
Wavelength	0.71073 Å	
Crystal system	Monoclinic	
Space group	$P2_1$	
Unit cell dimensions	a = 10.5225(4) Å	α= 90°
	b = 14.0033(5) Å	β= 109.949(5)°
	c = 11.3903(5) Å	γ = 90°
Volume	1577.65(11) $Å^3$	
Z	2	
Density (calculated)	1.418 Mg/m^3	
Absorption coefficient	0.757 mm^{-1}	
F(000)	698	
Crystal size	0.2 x 0.2 x 0.05 mm^3	
Theta range for data collection	2.91 to 28.48°.	
Index ranges	-13<=h<=9, -18<=k<=13, -12<=l<=15	
Reflections collected	7176	
Independent reflections	4885 [R(int) = 0.0312]	
Completeness to theta = 28.48°	83.2 %	
Absorption correction	None	
Refinement method	Full-matrix least-squares on F^2	
Data / restraints / parameters	4885 / 1 / 388	
Goodness-of-fit on F^2	0.719	
Final R indices [I>2sigma(I)]	R1 = 0.0309, wR2 = 0.0674	
R indices (all data)	R1 = 0.0412, wR2 = 0.0704	
Absolute structure parameter	0.013(15)	
Largest diff. peak and hole	0.317 and -0.304 $e.Å^{-3}$	

Table A-5. Crystallographic Data for $Fe^{III}(PS3)(CNC(CH_3)_3)_2$ (5)

Complex	**$Fe^{III}(PS3)(CNC(CH_3)_3)_2$**	
Empirical formula	$C_{28}\ H_{30}\ Fe\ N_2\ P\ S_3$	
Formula weight	577.54	
Crystal Color	Dark Purple	
Temperature	293(2) K	
Wavelength	0.71073 Å	
Crystal system	Monoclinic	
Space group	$P2_1/n$	
Unit cell dimensions	a = 11.0386(3) Å	α= 90°
	b = 11.9248(2) Å	β= 102.924(3)°
	c = 22.0505(6) Å	γ = 90°
Volume	2829.03(12) $Å^3$	
Z	4	
Density (calculated)	1.356 Mg/m^3	
Absorption coefficient	0.831 mm^{-1}	
F(000)	1204	
Crystal size	0.3 x 0.2 x 0.1 mm^3	
Theta range for data collection	2.86 to 29.63°.	
Index ranges	-15<=h<=14, -11<=k<=15, -30<=l<=17	
Reflections collected	16319	
Independent reflections	6782 [R(int) = 0.0358]	
Completeness to theta = 29.63°	84.9 %	
Refinement method	Full-matrix least-squares on F^2	
Data / restraints / parameters	6782 / 0 / 317	
Goodness-of-fit on F^2	0.761	
Final R indices [I>2sigma(I)]	R1 = 0.0323, wR2 = 0.0569	
R indices (all data)	R1 = 0.0759, wR2 = 0.0610	
Extinction coefficient	0.00000(15)	
Largest diff. peak and hole	0.283 and -0.234 $e.Å^{-3}$	